



TECHNISCHE
UNIVERSITÄT
WIEN

Vienna University of Technology

DIPLOMARBEIT

**Quantitative assessment of mitigation measures on
pedestrian thermal comfort within urban canyon**

unter der Leitung von

Univ.-Prof.Dipl.-Ing.Dr.techn. Ardeshir Mahdavi

E 259.3 Abteilung für Bauphysik und Bauökologie

Institut für Architekturwissenschaften

eingereicht an der

Technischen Universität Wien

Fakultät für Architektur und Raumplanung

von

Reza Nadianmehr

Matrkelnummer 1127147

Untere Augartenstraße 31 / Wien

Wien, Oktober 2015

ABSTRACT

Eine mögliche Strategie um urbane Wärmeinseln zu reduzieren ist die Implementierung von Gegenmaßnahmen wie Dachkühlung, Dachbefestigung und Begrünung. In dieser Arbeit wurde, mithilfe von Simulationssoftware, der Effekt verschiedener Maßnahmen auf die Reduktion von urbanen Wärmeinseln an einem Beispiel in Wien untersucht. In diesem Versuchsgebiet werden die absolute Lufttemperatur sowie die gefühlte Temperatur (Physiological Equivalent Temperature - PET), im Sommer (im Juli bei Sonnenuntergang) mit einem Beispielgebiet ohne Maßnahmenimplementierung verglichen. Das Ziel dieser Arbeit ist es jene Maßnahmen zu identifizieren, welche den größten Beitrag zur Reduktion der absoluten Temperatur sowie der gefühlten Temperatur leisten und somit das Wohlbefinden für die Stadtbewohner am effektivsten steigern. Die Studie soll Architekten und Stadtplanern helfen die Lebensqualität in Städten zu erhöhen.

ABSTRACT

One of the strategies that could help reduce urban heat islands is the implementation of various mitigation measures such as cool roofs, cool pavements and vegetation. For the purpose of the present research effort, the impact of a number of mitigation scenarios virtually implemented in a sample area in the city of Vienna has been assessed using the state-of-art numeric modelling tool. Air temperature and physiological equivalent temperature (PET) in summertime (in late afternoon in July) of envisioned mitigation scenarios will be compared with the base case, where mitigation measures are not implemented.

The aim of this work is to identify the cumulative effect of a number of mitigation measures that might increase the outdoor thermal comfort, thus affecting the PET, and decreasing the summertime air temperature. This study is expected to help architects and urban designers to improve the pedestrian thermal comfort.

ACKNOWLEDGMENT

I would never have been able to finish my dissertation without the guidance of my committee members, and support from my family.

I would like to express my deepest gratitude to my advisor, Prof. Ardeshir Mahdavi , for his excellent guidance, caring, patience, and providing me with an excellent atmosphere for doing research. I would like to thank DI Kristina Kiesel and Dr. Aida Maleki and Dr. Milena Vuckovic let me experience the research in the field and practical issues beyond the textbooks, patiently corrected my writing and supported my research.

CONTENTS

Table of Contents

1	INTRODUCTION	1
1.1	OVERVIEW.....	1
1.2	MOTIVATION	3
2	BACKGROUND	4
2.1	URBAN CLIMATE	4
2.2	STRUCTURE OF URBAN ATMOSPHERE	4
2.3	URBAN HEAT ISLAND (UHI).....	5
2.4	UHI INTENSITY	6
2.5	THE EFFECT OF UHI	7
2.6	MITIGATION	8
2.6.1	<i>Overview.....</i>	<i>8</i>
2.6.2	<i>Cool roof.....</i>	<i>8</i>
2.6.3	<i>Green Roof.....</i>	<i>12</i>
2.6.4	<i>Cool paving.....</i>	<i>14</i>
2.6.5	<i>Red road coating</i>	<i>17</i>
2.6.6	<i>Cooling with trees and vegetation.....</i>	<i>18</i>
2.7	OUTDOOR THERMAL COMFORT	23
2.7.1	<i>Overview.....</i>	<i>23</i>
2.7.2	<i>Outdoor comfort index</i>	<i>25</i>
2.7.3	<i>New effective temperature (SET).....</i>	<i>25</i>
2.7.4	<i>Predict Mean Vote (PMV).....</i>	<i>25</i>
2.7.5	<i>Physiological Equivalent Temperature (PET)</i>	<i>26</i>
2.7.6	<i>Comparison of thermal comfort indices</i>	<i>27</i>
2.8	APPLICATION TOOLS.....	27
2.8.1	<i>ENVI-MET.....</i>	<i>27</i>
2.8.2	<i>RAY-MAN</i>	<i>28</i>
3	METHOD	30
3.1	OVERVIEW.....	30
3.2	CASE STUDY	30
3.3	WEATHER DATA.....	31
	MODEL AREA	32
3.3.1	<i>ENVI-MET.....</i>	<i>32</i>
3.3.2	<i>RAY-MAN</i>	<i>33</i>

3.4	HYPOTHESIS.....	34
3.5	STATISTICAL ANALYSIS	35
3.5.1	<i>Simulation Input Data</i>	35
3.5.2	<i>Simulation Output Data</i>	35
3.6	SCENARIOS	36
3.6.1	<i>Basic model (BC)</i>	37
3.6.2	<i>First scenario (S1)</i>	38
3.6.3	<i>Second Scenario (S2)</i>	39
3.6.4	<i>Third scenario (S3)</i>	40
4	RESULTS.....	41
4.1	OVERVIEW.....	41
4.1.1	<i>DAY 1</i>	41
4.1.2	<i>DAY 2</i>	46
5	DISCUSSION	51
5.1	OVERVIEW.....	51
5.2	DAY 1.....	51
5.2.1	<i>Average difference of air temperature between BC and S1-S2-S3</i>	51
5.2.1	<i>Compared PET between BC and S1, S2 and S3</i>	52
5.3	DAY 2.....	53
5.3.1	<i>Average Difference of air temperature between BC and S1-S2-S3</i>	53
5.3.2	<i>Compared PET between BC and S1, S2 and S3</i>	54
6	CONCLUSION	56
7	INDEX	57
7.1	LIST OF FIGURES	57
7.2	LIST OF TABLES.....	59
7.3	LIST OF EQUATIONS.....	60
8	LITERATURE	61
8.1	REFERENCE	61
APPENDIX	67
A.1	ABBREVIATION	67
A.2	DAY 3.....	69
A.2.1	<i>Basic Model (without mitigation)</i>	69
A.2.2	<i>Physiological Equivalent Temperature on the Third Day</i>	70
A.2.3	<i>Average Difference air temperature between BC and S1-S2-S3</i>	73
A.2.4	<i>Compared PET between BC and S1-S2-S3</i>	74

1 INTRODUCTION

1.1 Overview

The aim of the present work is to investigate the influence of Urban Heat Island mitigation strategies on outdoor thermal comfort. For the purpose of this project an investigation in the urban area of Vienna was performed. Therefore, a street in the metropolitan area in Vienna has been selected.

Urban Heat Islands (UHIs) are a well-documented phenomenon (Oke 1969; Taha 1997; Voogt 2002; Wilby 2011; Kiesel et al. 2012; Mahdavi et al. 2014; Vuckovic et al. 2014). They are characterised by higher temperature of the urban area when compared to the respective rural area.

The development of human settlements leads to changes in natural landscapes. Moreover, today's urban domains are characterized by a dense morphology consisting of roads and buildings.

In general, there is abundance of sealed surfaces and lack of vegetative cover (EPA 2008). Changing from surfaces that were once moist and permeable generally become impermeable and watertight (EPA 2008). In addition, dark colours applied in building facades and pavements absorb more of the sun's energy (Gartland 2008).

Microclimate is a specific climate of a local atmospheric zone where the climate is different from the surrounding area (Mirzaie and Haghighat 2010). The minimum scale of this phenomenon can be a few square meters, for example a garden or a park and the maximum scale of this phenomenon can be several square kilometres. (Oke 2005).

Figure 1 shows the example profile of an urban area with regard to surface and air temperature.

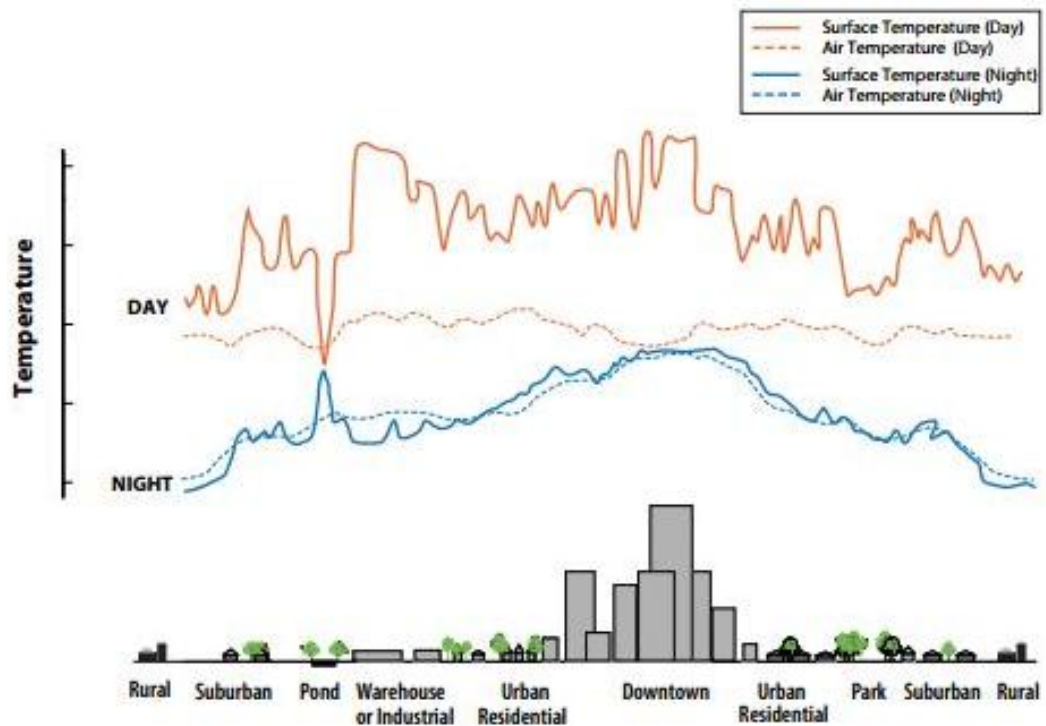


Figure 1: Variations of surface and Atmospheric Temperature (Munn 2001).

Urban heat Islands influence not only the energy consumption of the buildings but also the outdoor thermal comfort (Mirzaei and Haghighat 2010). To lessen the negative effect of the urban heat island various strategies can be applied within the urban domain that could lead to improve outdoor thermal comfort. This project focuses on the implementation and evaluation of different mitigation measures.

1.2 Motivation

At the moment, there is a worldwide tendency of population growth especially in urban areas. Therefore, more and more people are affected by the urban heat island phenomenon (Gartland 2008). Furthermore, the quality of urban areas is generally diminished due to the frequent occurrence of heat waves. Due to the fact that the outdoor spaces are essential part of the cities, as they integrate a number of activities (for example, pedestrian traffic or relaxing activities), and further contribute to the urban vitality and livability (Hakim et al. 1998, Hass-Klau 1993, Jacobs 1972, Whyte 1988), more frequent overheating influences lives of people every day. Moreover, higher temperatures within the urban areas are found to lead to an increased use of energy in buildings, due to the increased need for air conditioning (Magli et al. 2014, Morris and Simmonds 2000). Therefore, the first step of the present study is to underline the negative implications of the UHI. Additionally, a number of urban interventions are proposed, that may lessen the negative effects of the UHIs. Finally, these interventions are virtually implemented and their effectiveness evaluated via simulation. These insights will help guide the future urban planning resolutions and help integrate more climatically-aware urban design strategies.

2 BACKGROUND

2.1 Urban climate

Generally, urban climate refers to the climatic condition in an urban area that differ from neighbouring rural areas (Oke 2005). The main difference between urban and rural areas is the variation in surface cover. The surfaces in rural areas are mostly permeable, whereas urban structures are characterized by impermeable materials (EPA 2008). Building structure as well as the urban geometry are some of the most significant factors influencing the urban climate (Lindberg 2007). Other factors include the location of the city, anthropogenic heat production and pollution. According to Mills (1999) the urban climate is a research field where climatologist and designer have to ` together. In metropolitan areas many people are exposed to the adverse climatic effects and therefore it is important to understand the climatic influences and to be able to apply mitigation strategies in urban planning.

The microclimate, according to the MET Office (2011), is the specific climate of a small-scale area. This can refer to an area as small as a few m² up to a big park, a street, or a part of a city. This study will focus on the microclimatic variations on different streets within the city of Vienna. Furthermore the study will estimate outdoor thermal comfort using the PET index.

2.2 Structure of Urban Atmosphere

The lowest layer of atmosphere is called planetary boundary layer (PBL). The temperature, wind and moisture of this layer are directly influenced by the earth surface through the turbulence transfer of air mass .In urbanized region this layer is also called the urban boundary layer. The PBL is covered by a layer of warmer air which leads to creating temperature inversion (Encyclopædia Britannica Online 2015).

Current research has proven that there are significant differences in the boundary layers above rural and urban areas (Oke 1987). In rural areas during the night, the surface is cooler than the air above it, making a constant layer of cooler air below warmer air (Gartland 2008), whereas in urban areas during the night, urban surface that tend to slowly release the heat back to the surrounding air making it hotter which may result in an inversion layer forming above the canopy layer (Gartland 2008). The rural boundary layer is divided into the Surface Layer (SL) and Mixing Layer (ML), moreover the Urban Boundary Layer (UBL) is more complex as is shown in figure 2. It consists of the Urban Canopy Layer (UCL), which reaches from the ground to the average roof level, followed by Urban Roughness Sub layer (URS) and the Urban Mixing Layer (UML). (Erell et al 2011).

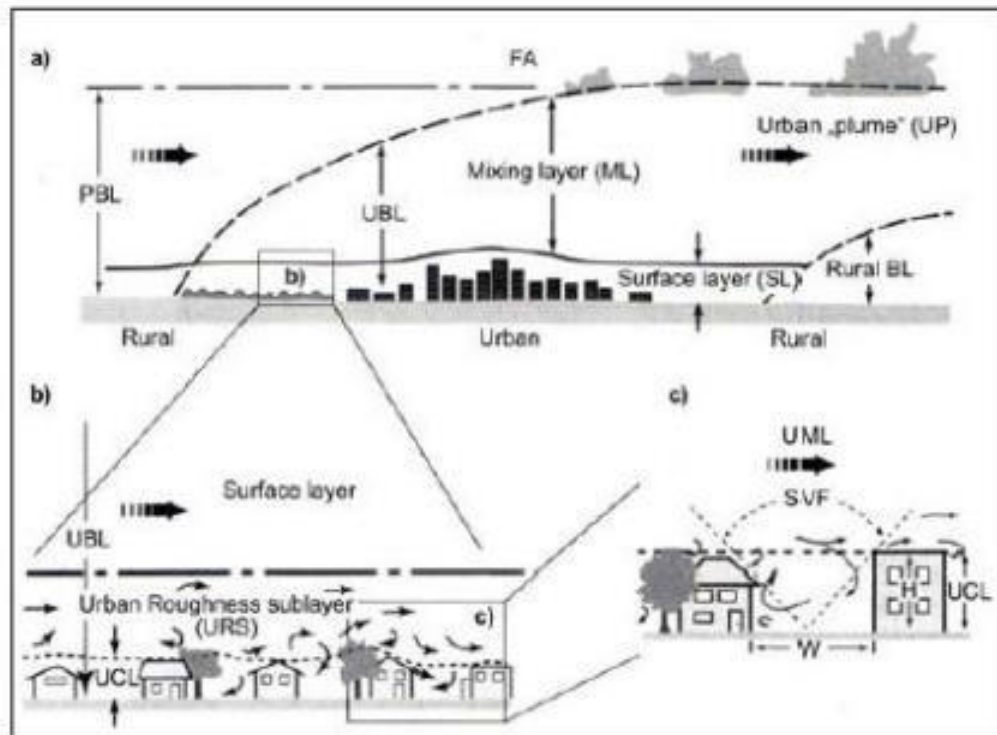


Figure 2: Modification by PBL by cities (Baely 1997)

2.3 Urban Heat Island (UHI)

Around half of the world population (3.4 billion) are inhabited in urban areas. Also, it is predicted that inhabitation in cities will reach more than 50% (5 Billion) by 2030 which means that additional two billion people will dwell inside cities by that year. Furthermore, the number of cities with population of over one million is expected to grow by nearly 100 from 2005 to 2015 (Population Reference Bureau 2005). Developing urban areas are the main aspect that lead to changes in natural environment. Across the world, the temperatures in urban areas are higher than of rural areas. This is usually the result of urban surfaces, namely of buildings and pavements, being impermeable and dry. In addition, they are able to absorb solar radiation and become extremely hot (Akbari 2005). The term Urban Heat Island describes this phenomenon. This phenomenon generally occurs in related area of human disturbance such as towns and cities (AMS Glossary of Meteorology 2000). Generally, the term urban heat Island is referred to relative warmth of air temperature near the ground (Oke 1982). Moreover, UHI forms due to a difference in cooling rates between urban and rural areas (Oke 1982). Figure 3 shows the diagram of urban heat island.

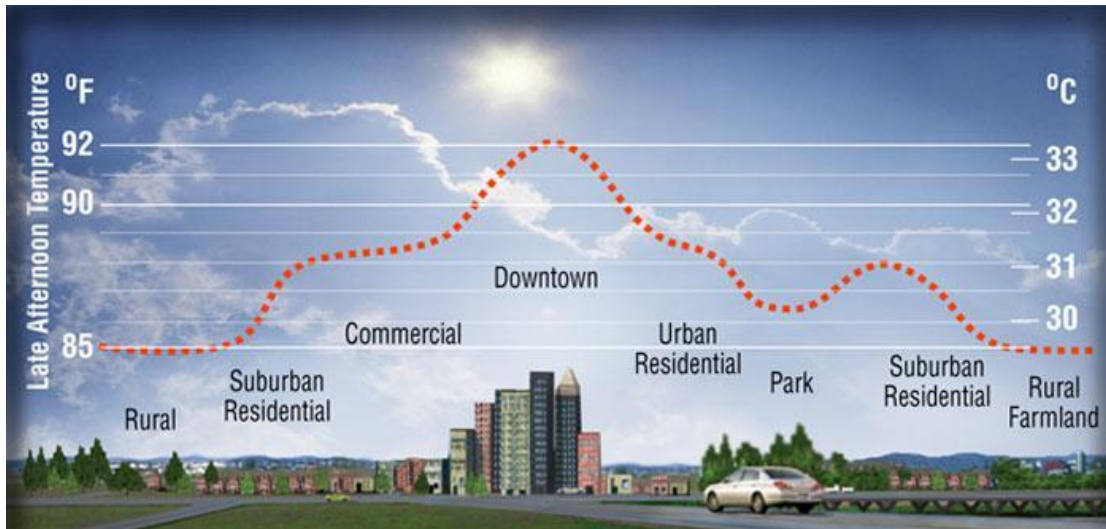


Figure 3: Diagram of the urban Heat Island (Image courtesy of Heat Island Group, Lawrence Berkeley National Laboratory)

2.4 UHI Intensity

The air temperatures of urban areas are higher than surrounding rural areas. The difference between urban and rural air temperatures is also called the heat island strength or intensity. It is often utilized to measure the magnitude of the heat island effect (Gartland 2008). The heat island intensity differs throughout day and night (Figure 4). Generally, the heat island intensity is the smallest in the morning and it is the largest at the night because during the night the urban surface continue to emit heat and slow the night-time cooling (Arnfield 2003, Gartland 2008). The magnitude of the UHI is increased in summer time and it leads to significant increase in air temperature and significant reduction in outdoor air quality. Furthermore, the buildings energy demand for cooling increases (Gartland 2008, Mirzaie and Haghighat 2010). According to Moll and Berish (1996) the peak heat island magnitude as large as 7K have been recorded which is usually happening three to five hours after sunset (Oke 1987).

The following equation (1) shows calculation of the urban heat island intensity (Oke 1982)

$$\Delta T = T_{urban} - T_{rural} \quad (1)$$

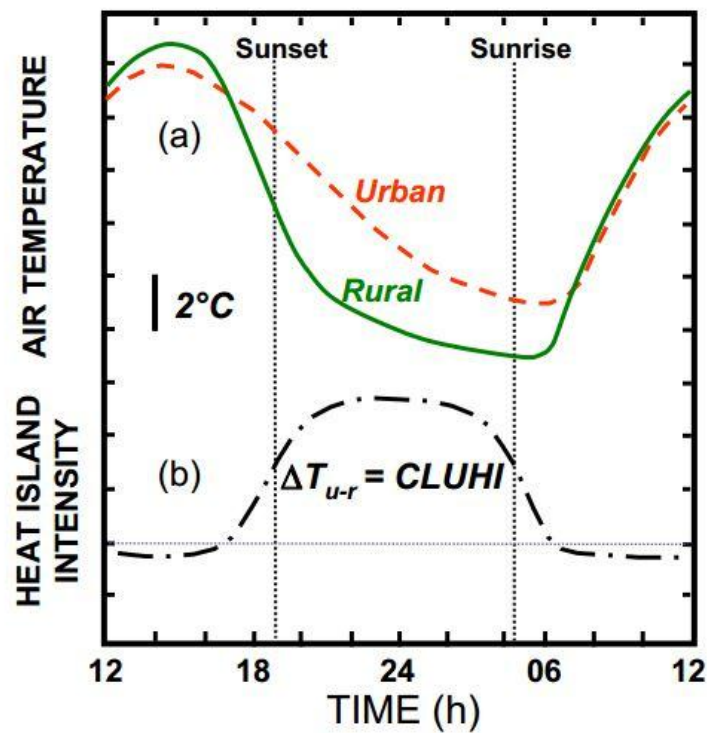


Figure 4: The diagram of intensity of UHI (Oke 1982)

2.5 The Effect of UHI

On the basis of the studies currently available (for example , Morris and Simmonds 2000 , EPA 2008, Gartland 2008), the annual mean air temperature of a city with one million people or more inhabitants can be 1 to 3K warmer than rural areas on a clear, calm night. This temperature difference can get up to as much as 12K. Therefore, increased temperatures from urban heat islands especially during the summer have a negative impact on quality of life and community's environment such as:

- Increased energy consumption
- Elevated emission of air pollutants and greenhouse gases
- Compromised human health and comfort
- Impaired water quality. (Morris and Simmonds 2000 , EPA 2008, Gartland 2008)

2.6 Mitigation

2.6.1 Overview

Currently, numerous UHI mitigation strategies exist to lessen the negative effects of the urban heat island effect. A number of studies focused on the various ways that could lead to reduction of the urban heat Island effect:

According to Mirzaie and Haghighat (2010) increasing the material's albedo in cities and increasing the amount of trees, vegetation and ponds within urban area can decrease UHI. These strategies have direct and indirect effect on reduction of air temperature, energy consumption and increase outdoor air quality. Developing green space, planting trees and using the materials with higher albedo for roof, pavement, as well as, motor way could lead to reduction of UHI within the canopy layer. Furthermore, the geometry of the buildings, the orientation of the buildings, the ratio of height of the buildings to width of the street (H/W), the ratio of the height of the buildings to length of the street (H/L) among others (Mills 1999, Oke 1988) are another strategies that could lead to the reduction of UHI. The aim of this study is to introduce and explain cool roof and cool paving and vegetation as mitigating solutions and study their influences in reducing of air temperature and increasing outdoor air quality in microclimate.

2.6.2 Cool roof

Generally, most important characteristic of a Cool roof material is staying cooler when the sun is shining (Gartland 2008). Normally, cool roofs may heat up to about 40 to 60 °C, whereas traditional roof systems may reach values of 50 to 90 °C (Gartland 2008). Beside this, traditional roofing materials have negative effects for the buildings such as:

- Increasing indoor temperature
- Increasing energy supply used for cooling
- Decreasing indoor comfort
- Using traditional roof materials can lead to higher urban and suburban temperatures (Gartland 2008).

The two most important properties of cool roof materials are high solar reflectance (Albedo) and high thermal emittance (Emissivity). Albedo describes the ability of a surface to reflect solar energy. It is measured on a scale from 0 to 1, a higher value refers to a higher solar reflectance (Albedo) (Medgar et al. 2007). Traditional roofing materials have an albedo of 0.5-0.25, whereas cool roofs should have an albedo above 0.7 (Gartland 2008). Thermal Emissivity

describes the percentage of solar energy that material is able to radiate back to the environment. Materials with high thermal emittance are able to release heat faster and therefore stay cooler. This index is measured in percent from 0-100 (Medgar et al. 2007). According to the Gartland (2008) the thermal reflectance of a white roof is 75% and thermal emittance is 92% percent whereas, the thermal reflectance and thermal emittance in traditional roofs are 5-25% and over 80% respectively. Figure 5 shows the combined effects of solar reflectance and emittance on roof temperature (Gartland 2008).

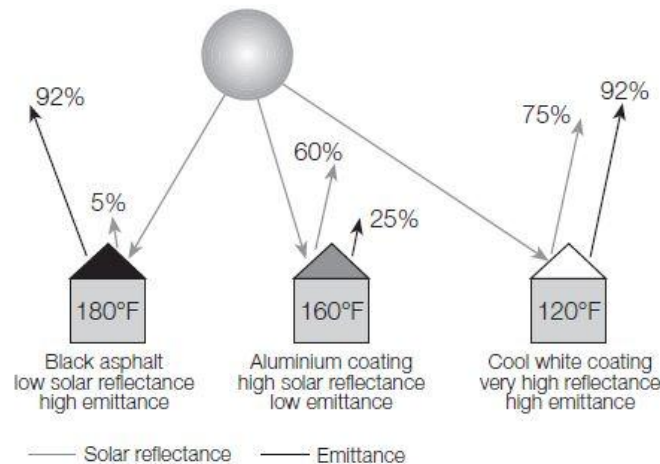


Figure 5: The effect of solar emittance and solar reflectance on roof temperatures (Gartland 2008)

Generally, total amount of solar energy that is reaching the earth's surface is higher on clear summer day. Ultra-violet (UV) rays, visible light and infrared energy are all components of solar energy that are reaching the Earth in different amounts (Gartland 2008). These studies show that Ultra-violet (UV) rays make up 5 percent, visible light make up 43 percent, in colors ranging from violet to red, infrared energy make up 52 percent which is perceived as heat (Figure 6) (EPA 2008).

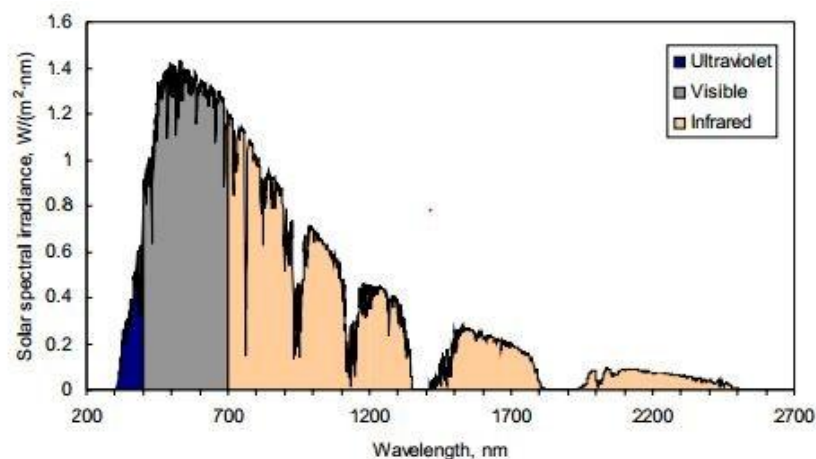


Figure 6: Spectrum of solar radiation (EPA 2008)

Benefits and negative effect of cool roofs

Cool roofs have positive effects in different aspects such as: Urban Heat Island Mitigation, improving building comfort, public health benefits, peak energy savings and grid stability (Gartland 2008, EPA 2008).

A white roof can be suitable to a buildings for many reason:

- Reducing the energy bills by decreasing air conditions needs
- Improving indoor thermal comfort for space
- Decreasing roof operating temperature

In many cases the cost of cool roofs are same as non-cool alternative. Moreover, the energy cost saving of a cool roof depends on multiple factors, including local climate, the amount of insulation in roof and function of the buildings and etc. Cool roofs have a surface that reflect the sunlight and emit heat more efficiently than traditional roofs (Urban and Roth 2010). The cool roofs are constituted of one or more different materials Differing roofing structure shows different surface option.

Beside the many advantages of cool roofs, these materials have a winter time heating penalty (Gartland 2008).Cool roofs able to reflect beneficial heat that could warm the building in winter time (Figure 7). Although, in the most urban climates this penalty is not big enough to cancel out the summertime saving. There are two reasons: first, in wintertime the sun is much weaker and there are fewer daylight hours. Second: in winter time natural gas is used for heating (Gartland 2008).

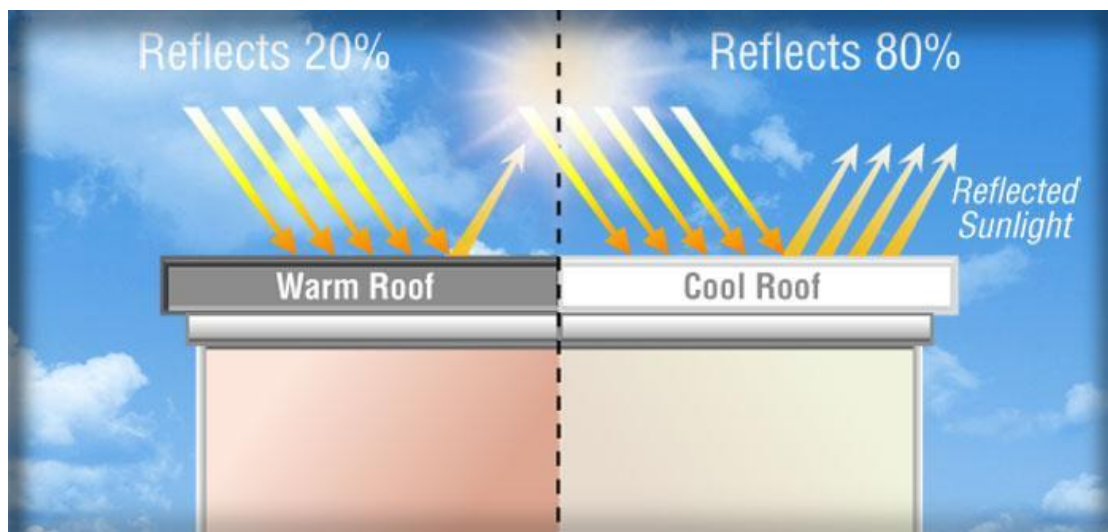


Figure 7: Comparing white roof and traditional roof (Image courtesy of Heat Island Group, Lawrence Berkeley National Laboratory)

Type of cool roof

Cool Roof Coatings: contain white or special reflective pigments that reflect sunlight. Coatings are very thick paints that can protect the roof surface from ultra-violet (UV) light and chemical damage, and etc. (Urban and Roth 2010).

Built-Up Roofs: the structure of this type of cool roof is a base sheet, fabric reinforcement layers, and a protective surface layer that is traditionally dark (Urban and Roth 2010). The surface layer can be made in a few various ways, and each has cool options. One way involves embedding mineral aggregate (gravel) in a flood coat of asphalt. By substituting reflective marble chips or gray slag for dark gravel can make the roof cool. A second way of built-up roofs are finished with a mineral surfaced sheet. These can be made cool with reflective mineral granules or with a factory-applied coating. Another surface option involves coating the roof with a dark asphaltic emulsion. This type can be made cool by applying a cool coating directly on top of the dark emulsion (Urban and Roth 2010).

Tile Roofs: this type of cool roof is made of clay, slate, or concrete. Clay and slate tiles come from the terrain, so their colors vary depending on the earth's composition. Some varieties will naturally be reflective enough to achieve cool roof standards. Tiles can be also be glazed to provide waterproofing or coated to provide customized colors and surface properties. These surface treatments can transform tiles with low solar reflectance into cool roof (Urban and Roth 2010). Figure 8 shows two different type of installation of white roof.



Figure 8: Two different type of installation of white roof

Single play membrane (right) and Coating (Right) (Urban and Roth 2010)



2.6.3 Green Roof

Green roofs are another type of cool roof. A green roof is fundamentally a garden grown on the roof (Gartland 2008) (Figure 9). Extensive green roof and intensive green roof are two main types of green roof system (Gartland 2008). Table 1 shows the comparison between intensive and extensive green roof.



Figure 9: The different type of Green Roofs (Green business watch 2013)

Table 1: The type of Green roofs and their properties as briefly.

Cool Roof Type	Type	Shape	Properties
Green Roof	Intensive		Maintenance: High Irrigation: Regularly System build-up height: 150-400mm Weight: 180-500kg/m ² Cost: High Use: Park like garden (Gartland 2008)
	extensive		Maintenance: Low Irrigation: No System build-up height: 60-200mm Weight: 60-150kg/m ² Cost: low Use: Ecological protection layer (Gartland 2008)

In this project, extensive green roof (Figure 10) is more useful than an intensive green roof because the weight of an extensive green roof is lower than an intensive green roof, as well as, this system can be grown on roofs with slopes of up to 30° (Gartland 2008). In addition, it is covered with grass (Gartland 2008). In this project the grass with 50 cm length have been assigned as covering for the extensive green roof (Figure11).

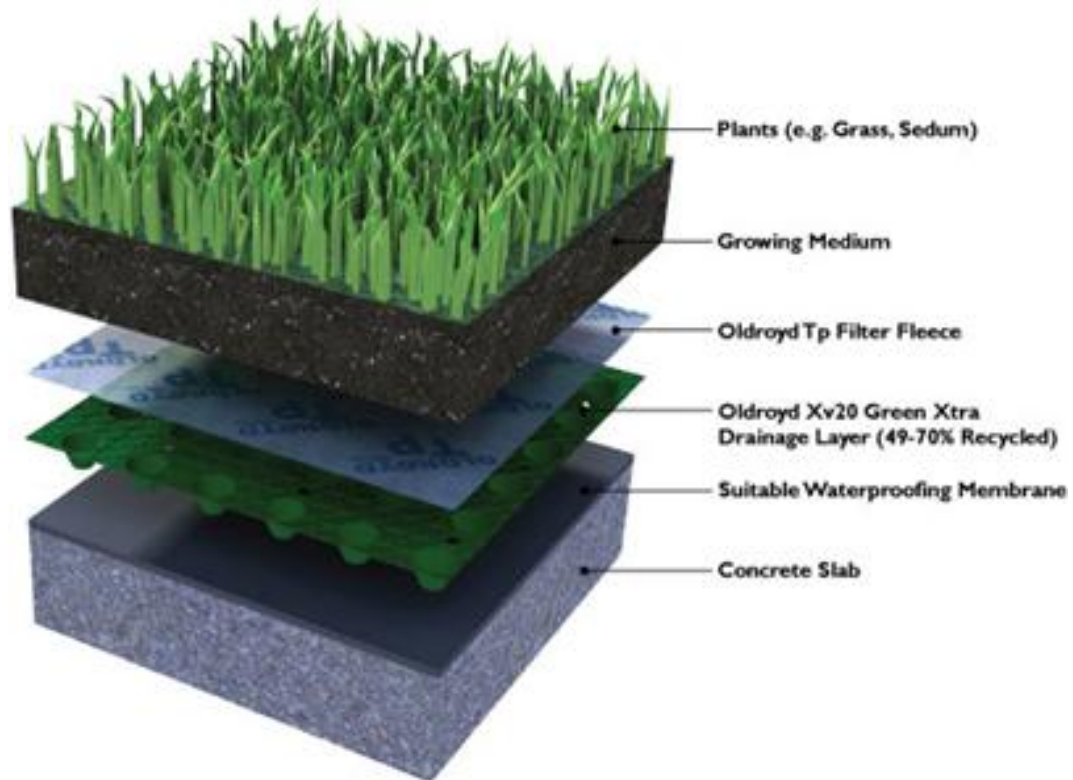


Figure 10: Extensive Green roof (SAFEGUARD 2012)

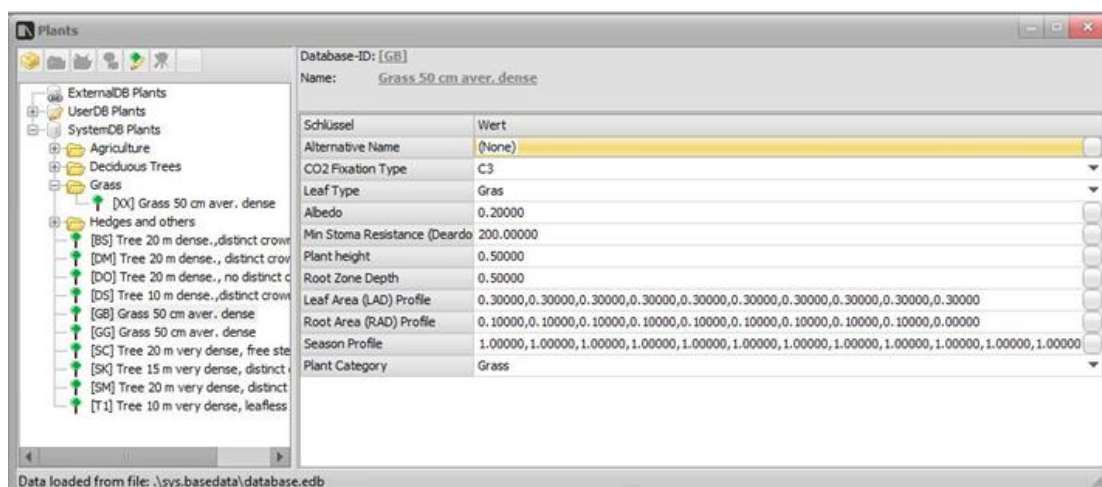


Figure 11: The properties of Grass (Bruse 1999)

Benefits and negative effects of green roofs

On the basis of the studies currently available, it seems fair to suggest that green roofs have been mentioned as one of as suitable strategy most effective strategy for UHI mitigation, energy saving and air quality.

In recent studies have identified that the green roofs have advantage in energy-conservation and cooling at the building scale. In addition, they can reduce the air temperature by around 2.8 K on an urban scale. (Bass et al. 2002, Gartland 2008). Another advantage of green roofs are energy saving in the building. This means that less heat is transmitted from the roof into building by increasing insulation (soil and roof system layer) (Gartland 2008). Beside this, green roofs also have negative effect in compare in traditional roof:

- Costs – depending on the type, the initial costs and maintenance of green roofs can be rather expensive
- Construction – depending on the type and use of green roofs, the weight of the construction has to be considered.

2.6.4 Cool paving

The high percentage of suburban and rural areas is covered by sealed surfaces (Gartland 2008). Additionally, around 40 percent of total urban space constitute of pavements (Akbari et al. 2008). Paved areas tend to absorb and store, as well as, release the largest part of the sun's energy, which is contributing to the heat island effect (Gartland 2008).

Generally, properties of hot pavement pertain to:

- Impermeability
- Dark in colour
- The amount of solar reflectance under 25 percent (Gartland 2008).

These pavements are able to achieve the rise of temperature up to 65°C or more in the summer, whereas using the cool paving can lead to reduction of temperature to 15°C or more (Asaeda et al. 1996, Pomerantz et al. 2000, Gartland 2001).

Based on these studies it can be concluded that there are two ways to create a cool pavement:

1. Increasing the value of their solar reflectance:

This means creating pavements that have brighter color by using lighter colored component and applying lighter coating over the pavement surface (Gartland 2008). Figure 12 shows comparing cool pavement and dark pavement aspect of their solar reflectance in urban heat island.



Figure 12: Compared cool pavement and dark pavement (Image courtesy of Heat Island Group, Lawrence Berkeley National Laboratory)

2. Increasing their ability to store and evaporate:

Making porous pavements by raising the ability of them to store water. Porous pavements are able to drain better through during rainstorm and evaporate better during hot and sunny weather (figure 13). In general, the value of thermal emittance is not important factor affecting the pavement temperature (Gartland 2008).



Figure 13: porous pavement (Haus and Wohnen 2011)

Properties of Light concrete pavement aspect of UHI

Generally, the main features of conventional pavements include: their tendencies to be impermeable and their dark color so that, the value of thermal reflectance in this type of pavements is lower by 25 percent (Gartland 2008). Whereas, cool paving is able to reduce the pavement temperature by 19.5 °C (Figure 14) (Asaeda et al. 1996, Pomerantz et al. 2000, Gartland 2001). Therefore the value of thermal reflectance and thermal emittance are the most important factors of cool pavement aspect of Urban Heat Island (Gartland 2008). The value of thermal reflectance is higher than 80 percent and thermal emittance is between 80 and 90 percent. According to Gartland (2008) the value of thermal emittance is not important factor in the surface temperature of pavement as material used for roofing (Gartland 2008). Concrete pavements have solar reflectance values ranging between 70 and 90 percent. Figure 15 shows the properties of cool paving through software.



Figure 14: Cool paving (BerkeleyLAB)

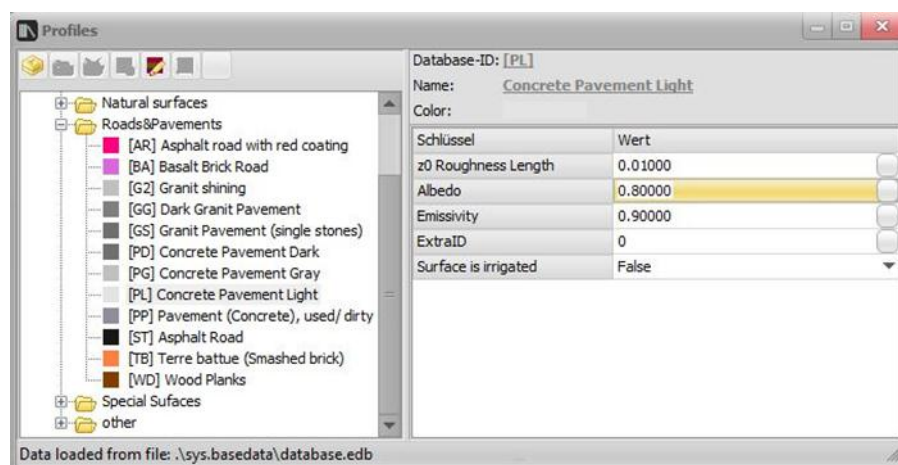


Figure 15: Properties of cool paving (Bruse 1999)

2.6.5 Red road coating

The material of asphalt pavement is generally a mixture of crushed stone with some sand and performance together by a thick sticky liquid petroleum product (Figure 16) (Furth 2012). Considerable, bitumen is sticky liquid petroleum, which is called in the UK and similarly asphalt in the U.S.A normal asphalt has black color, which gives the pavement its color refineries also make clear bitumen (Furth 2012).



Figure 16: Red road coating (Fietsberaad crow 2011)

In this project, red road coating has been assigned to in the second scenario for motor way. The value of albedo is about 0.5 (Figure 17), whereas the value of albedo for regular asphalt (Black asphalt) is about 0.2 (Figure 18).

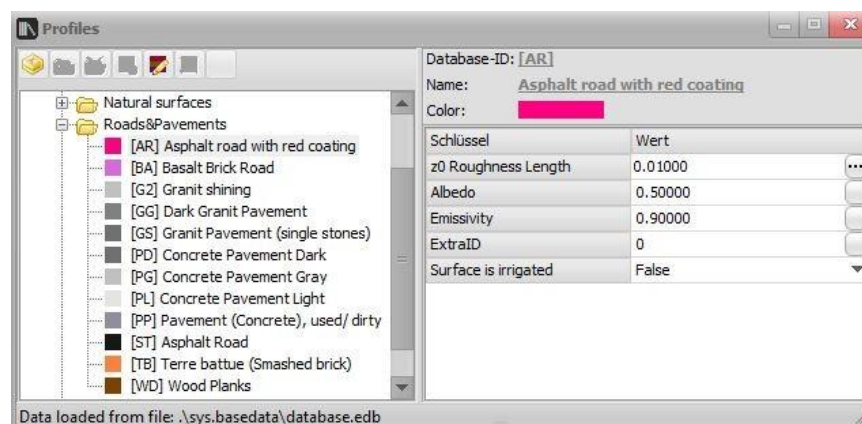


Figure 17: The properties of asphalt road with red coating (Bruse 1999)

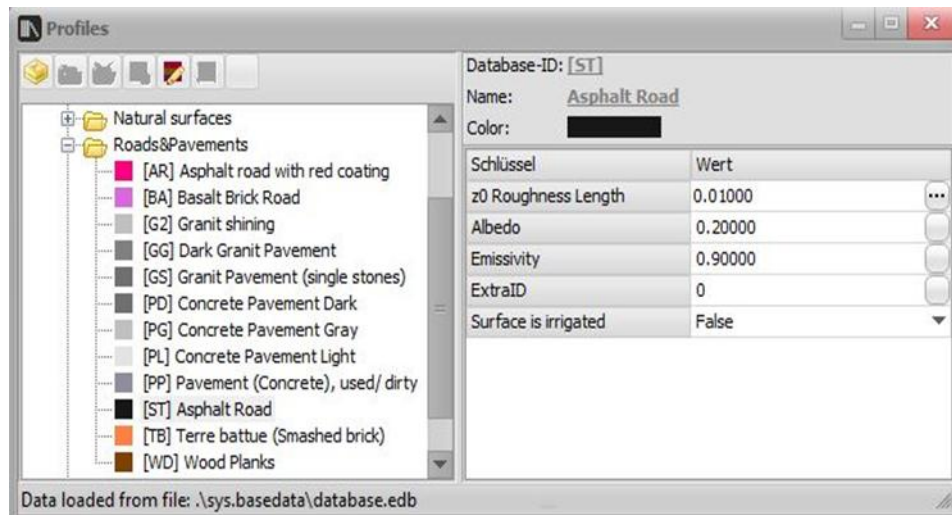


Figure 18: The properties of regular asphalt (Bruse 1999)

Advantages of asphalt with red coating

One of the main reasons for using this type of asphalt regarding the issues of Urban Heat Islands is that it has the high thermal reflectance in comparison to regular asphalt. The thermal reflectance (Albedo) of asphalt with red coating is between 0.4-0.5, whereas the thermal reflectance in black asphalt is 0.2 (Furth 2012).

The cost of asphalt with red coating

To make colored asphalt pavement, there are three main changes obligatory in the construction. For instance how much of each elements are going to add to the mix. Such as: colorant, red stones, clear asphalt. Clear asphalt is the most common element, with 2% pigment and pink stones and costs 4 to 5 times more than regular black asphalt per to (Furth 2012).

2.6.6 Cooling with trees and vegetation

Trees and vegetation are the most essential components of a healthy city (Gartland 2008). They could cover an additional 15 percent of the city, increasing shading to 20 percent of roof and road, 50 percent of the sidewalk, as well as 30 percent in parking lots. (Akbari and Rose, 1999). Planting trees and vegetation has several benefits such as: more comfortable communities, lower energy use, reduced air pollution, decreased storm water run-off, as well as, an improved ecosystem (Gartland 2008).

Trees and vegetation can help reduce urban heat island effect in two ways: first shade, leaves and branches can shade the buildings and pavement, thus keeping the surface cooler. In addition, they can reduce the heat transferred to the air. One of the most useful benefits from the shade of trees is that it can protect people from the sun's ultraviolet rays (Gartland 2008). Second aspect is evapotranspiration (Figure 19) that keeps the surrounding air cool. The evapotranspiration reduces air temperature within and downwind of well-vegetated areas (Gartland 2008).

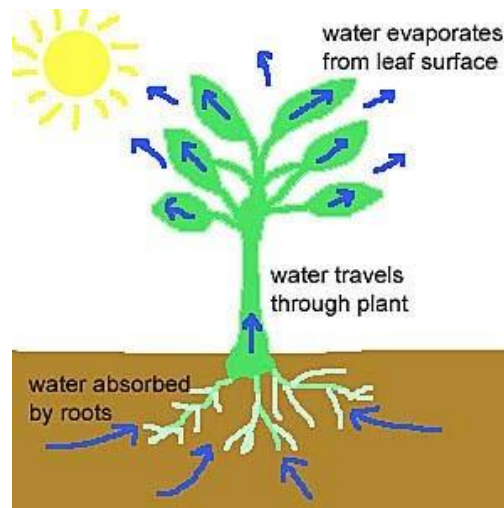


Figure 19: Evapotranspiration (Garden Punk 2012)

Reduced Heat islands and more comfortable communities

Shading and evapotranspiration are two aspects of trees and vegetation that lead to improvement in the outdoor comfort and reduction of the heat islands (Huang et al. 1990). Generally, the amount of radiation transmitted differs with the type of tree (Gartland, 2008). In summer the amount of overall radiation transmitted through the tree crown is between 6 and 30 percent, whereas the amount of radiation transmitted will be increased between 8 and 10 in winter (Huang et al. 1990). Shading may help reduce the peak summer temperature by 5-20 °C (Meier 1990). Therefore, the cooler surface leads to reduction of heat transmitted to the surrounding air (Gartland 2008). The process of absorbing water through roots of trees and vegetation and emitting it as vapor through their leaves is called evapotranspiration. Evapotranspiration can reduce air temperature in hot summer periods. In addition this process increases the moisture and raise the amount of humidity (Gartland 2008). Based on conducted studies thus far, it is also revealed that implementing trees leads to reduction of wind speed by 20-80 percent, depending on the density of the canopy (Gartland 2008). The trees shielding is proved to be the most beneficial when blocking cold northerly wind in the winter.

Advantage of planting trees

Planting trees around the buildings has three beneficial effects:

1. Trees able to reduction the maximum temperature of a building by shading walls and windows from the sun.
2. Trees block winds, which tend to reduce in winter heating costs and potentially increases summertime cooling needs
3. Trees lead to reduced air temperatures around the buildings which is most useful during the summer (Gartland 2008).

Species of trees

The trees and vegetation can be most beneficial, when planted in strategic location around the building (McPherson et al. 1999). In addition, species of trees have significant effect on reduction energy consumption in the building and increasing air quality in the canyon layer. For example, planting deciduous species (Figure 20) to the east, southeast, south and southwest have the most effect for cooling buildings. Furthermore, planting evergreen (conifers) specious (Figure 21) to the north of the buildings block winter winds (Gartland 2008). According to this case study, it is shown that when positioning the trees and vegetation to the north and south of the buildings the positive effect in air temperature reduction is far greater (Figure 22 and figure 23)

Table 2 shows the impact of each mitigation in different type as separately and it describes the expected result before the simulation is conducted.



Figure 20: Two types of deciduous trees

Left: *Tilia cordata* tree Plams Present and Right: *Castanea* (variety of life 2014)



Figure 21: Type of coniferous (NukeCZ 2010)

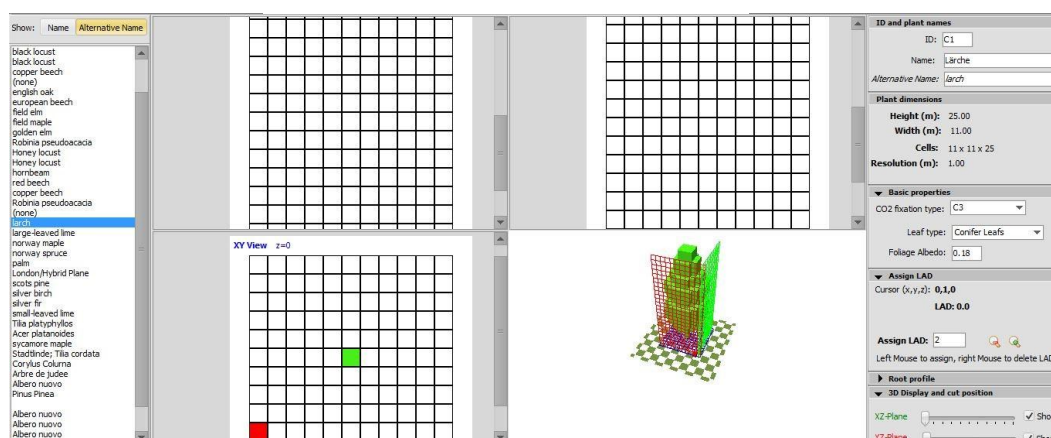


Figure 22: Properties of conifer trees (Bruse 1999)

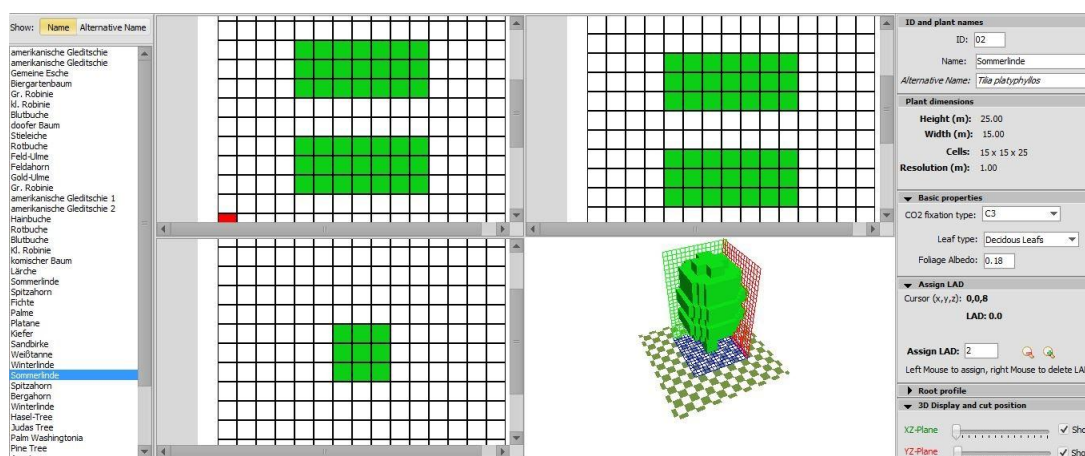


Figure 23: Properties of deciduous trees (Bruse 1999)

Table 2: The impact of each mitigation and expected results prior to simulation.

Element	Type		properties	expecting results before simulation	Note
vegetation	V1=Tress	deciduous	-plant in south, to create shad(Gartland 2008)	-Improving outdoor comfort -Decreasing air pollution -Reduce air temperature -Increase humidity	Fraxinus excelsior: growing to 20–35 m trunk up to 2 m diameter leaves are 20–35 cm long Tilia: growing to 20–40 m trunk up to 1 m diameter leaves are 3–8 cm long
		conifers	-plant in north , tend to block cold winter winds (Gartland 2008)		
	V2=Grass	Different type	-		
paving	P1= Lighter in color	Thermal emittance >80%	-The largest effect on solar reflectance.	Reduced air temperature Decreased air pollution	Two way to make pavements cooler: by Incresing solar reflectance And By increasing thier ability to store and evaporate water
	P2=Pervious (permeable)		-Usually use for pedestrian path -Low durability for Roadway path		
Roof	R1=White Roof	Solar reflectance>70% High thermal emittance	-Cheaper than green roof -The maintenance cost is lower than green roof	Reduced air temperture	materials need to have both: High thermal reflectance High thermal emissivity
	R2=Green Roof	extensive	Solar Reflectance > 40%	Reduce air Temperature	
		intensive		Increase humidity	

2.7 Outdoor Thermal Comfort

2.7.1 Overview

Outdoor thermal comfort is discussed as one of the essential topics connected with the urban climate and increased heat stress (Chen and Ng 2011, Honjo 2009). Based on this, during the last decades, climate change and increased heat stress are of higher interest when conducting an evaluation of outdoor thermal comfort (Chen and Ng 2011, Honjo 2009).

Properly designed outdoor spaces can lead to more sustainable cities if the climatically aware design strategies are applied (Matzarakis and Amelung 2008). Majority of people are using outdoor public spaces, such as streets, thus they need to satisfy different aspects, such as, environmental, economic and social aspect (Chen and Ng 2011, Honjo 2009).

Factors affecting the indoor temperature and the outdoor temperature are different. While the indoor air conditions can be maintained within the comfort limits, energy balance of the human body adapts to the outdoor environment (Matzarakis and Amelung 2008). Based on studies done in this field, it can be concluded that the outdoor thermal comfort indices, such as Standard Effective Temperature (SET), Predict Mean Vote (PMV) and physiological equivalent temperature (PET) are the most important and commonly used indices (Honjo 2009). Table 3 lists the indexes used in thermal comfort evaluation studies for indoor and outdoor environments.

Table 3: Scaled thermal comfort indices for indoor and outdoor (Fanger 1970, Givoni 1976 , ASHRAE 2001 and Toudert 2005)

Index	Definition
<i>Empirical indices</i>	
ET Effective Temp.	Set in monograms and represent the instantaneous thermal sensation estimated experimentally as combination of T_a , RH and v
RT Resultant Temp.	Comparable to ET but tested for a longer time to meet assumed thermal equilibrium
HOP Humid Operative Temp.	Temperature of uniform environment at a relative humidity RH=100% in which a person loses the same total amount of heat from skin as the actual environment (comparable to ET * but RH equals 50% for HOP)
OP Operative Temp.	Arithmetic average of T_a and T_{mrt} ,that is including solar and infrared radiant fluxes weighted by exchange coefficient
WCI Wind Chill Index	Based on the rate of heat loss from exposed skin caused by wind and cold and is function of T_a and v ;suitable for winter condition
<i>Rational indices</i>	
ITS Index of Thermal Stress	Assumes that within the range of conditions where it is possible to maintain thermal equilibrium, sweat is secreted at sufficient rate to achieve evaporative cooling.
HSI Heat Stress Index	Ratio of the total evaporative heat loss E_{sk} required to thermal equilibrium to the maximum of evaporative heat loss E_{max} possible for the environment , for steady –state conditions ($S_{skin}=S_{core}=0$) and $T_{sk}=35$ °C constant
ET* New Effective Temp.	Temperature of a standard environment (RH=50%, $T_a=T_{mrt}$, $v < 0.15$ ms ⁻¹) in which the subject would experience the same sweating SW and T_{sk} as in the actual environment. It is calculated for light activity and light clothing
SET* Stand. Effective Temp.	Similar to ET* but with clothing variable. Clothing is standardized for activity concerned.
OUT_SET Out.Stand.Eff.Temp.	Similar to SET* but adapted outdoors by taking into account the solar radiation fluxes .reference indoor conditions are $T_{mrt}=T_a$;RH=50%; $V=0.15$ ms ⁻¹
PMV and PT Predict mean vote Perceived Temp	PMV express the variance on a scale from .3 to +3 from a balanced human heat budget and PT the temperature of a standardized environment which achieve the same PMV as the real environment. Clothing and activity are variables.
PET Physio. Equiv. Temp.	Temperature at which in a typical indoor setting : $T_{mrt}=T_a$;VP=12hp ; $v=0.1$ ms ⁻¹ , the heat balance of the human body (light activity , 0.9 clo) is maintained with core and skin temperature equal to those under actual conditions unity °C.

2.7.2 Outdoor comfort index

The evaluation of the human thermal comfort is not a new topic. People have always been concerned by their well-being and looked for methods to quantify their sensation of cold or heat (Matzarakis and Amelung 2008). The thermal environment and its impact on human is multidimensional and it cannot be explained as a function of one individual factor, such as air temperature (T_a), because the body contains many various sensors for each factor (Matzarakis and Amelung 2008).

In this chapter the following indices will be explained:

- Standard Effective Temperature
- Predict Mean Vote
- physiological equivalent temperature

2.7.3 New effective temperature (SET)

The new effective temperature is an index of outdoor comfort which is based on human energy balance. This index can be compared with conditions in standardized room. In this index the mean radiant temperature is equal to air temperature, as well as, a constant relative humidity of 50% (Fanger 1970). New effective temperature is similar to effective temperature, however, here the clothing is used as a constant value for outdoor activities. Also, SET may be used to calculate both indoor and outdoor comfort levels. In recent studies, the distribution of this index is calculated and assessed as the output of computational fluid dynamic (CFD) software (Fanger 1970).

2.7.4 Predict Mean Vote (PMV)

This index was developed by Fanger in 1970 and it is widely employed in the realm of climate studies. This index is constituted of four physical variables (air temperature, relative humidity, wind speed and mean radiant temperature) and two personal variables (clothing insulation and activity variable). Furthermore, this index provides a value that corresponds to the ASHRAE thermal sensation scale and demonstrates the average thermal sensation by a large group of people in an area. Table 2 shows the range of this index (ASHRAE 2001, Fanger 1970). For the purpose of defining the range and related sensation, the participants were dressed in standardized clothing and completed standardized activities while exposed to different thermal environments.

2.7.5 Physiological Equivalent Temperature (PET)

The bases of this index is the thermo–physiological heat balance model which is called the Munich energy balance model for individual (MEMI). According to Matzarakis and Amelung (2008) PET is defined as the equivalent air temperature at which in a typical indoor conditioned heat balance of the human body exists; work metabolism 80 W of light activity, and clothing of 0.9 clo. The following assumption is made for indoor reference climate (Matzarakis and Amelung 2008):

- The amount of mean radiant temperature equals air temperature ($T_{mrt}=T_A$).
- The value air velocity (Wind speed) is constant to 0.1 m/s.
- Water vapor pressure is fix to 12 hPa (approximately equivalent to a relative humidity of 50% at T_A 20°C).

RAY-MAN as a software able to calculate the PET index which is developed by Matzarakis and his team in meteorological Institute Freiburg of Germany (Matzarakis and Amelung 2008). Table 4 shows the range of PMV and PET for different levels of thermal perception and physiological stress.

Table 4: Range of PMV and PET for different grade of thermal perception and physiological stress (Matzarakis and Mayer 1996)

PMV(°C)	PET (°C)	Thermal Perception	Grade of Physical stress
		Very cold	Extreme cold stress
-3.5	4	Cold	Strong cold stress
-2.5	8	Cool	Moderate cold
-1.5	13	Slightly cool	stress
-0.5	18	Comfortable	Slight cold stress
0.5	23	Slightly warm	No thermal stress
1.5	29	Warm	Slight heat stress
2.5	35	Hot	Moderate heat stress
3.5	41	Very hot	Strong heat stress
			Extreme heat stress

2.7.6 Comparison of thermal comfort indices

SET takes two factors as variables: first, activity and second, clothing insulation(I_{clo}), which means that the human adaptive behavior is included, whereas these factors are kept constant in physiological Equivalent Temperature (PET), which means, just the thermal environment is assessed (Toudert 2005). OUT_SET is similar to SET but when calculating this index, it is essential to know the amount of solar radiation fluxes (Toudert 2005). The value of relative Humidity is $RH=50\%$ in OUT_SET index which is changing with T_A . The PET is believed to be more accurate than OUT_SET; the amount of vapor pressure is equal 12 hPa which is constant in the air independent from air temperature.

2.8 Application Tools

2.8.1 ENVI-MET

Overview

According to ASHRAE (2005), Computational Fluid Dynamic (CFD) models are able to resolve the air flow around a building by following the Navier-Stokes equation at the finite grid situations. In addition, CFD models are currently very powerful model methods in view of calculating internal flow, although additional validation with actual measured data is needed to test the reliability of the simulation output. In the following paragraphs ENVI-MET will be introduced as a CFD tool used to perform simulations of this project.

Introduction

„[...]ENVI-MET is a three-dimensional micro-climate model designed to simulate surface – plant –air interaction in urban environments with a typical resolution of 0.5 to 10m in space and 10 sec in time. Typical areas of application are urban climatology, Architecture, Building Design, or Environmental planning, just to name a few” (Bruse 1999). Additionally, it is a prognostic model and it is based on fundamentals of fluid dynamics. This software is capable to simulate:

- The flow around and between buildings
- The exchange process of heat and vapor at the ground surface and at walls
- Turbulence
- Exchange at the vegetation and vegetation parameters bioclimatology
- Pollution Dispersion (Bruse 1999).

Advantages of using ENVI.MET

Generally, the use of ENVI-MET has many advantages and some of them are mentioned below (Toudert 2005):

- Simulating the micro-climatic dynamics within daily cycle. The model is prognoses in-stationary and non-hydrostatic, as well as, all exchanges including humidity, temperature, wind flow turbulence and radiation fluxes.
- The representing of complex urban structure. I.e. buildings with various height and shape. In addition the vegetation is handled not only as a porous obstacle to wind and solar radiation, but also by including the physiological processes of evapotranspiration and photosynthesis, as well as, different type of vegetation and specific properties can be used etc.
- Clear Readings of the micro-climate changes by high spatial resolution (up to 0.5 m horizontally) and the high temporal resolution (up to 10 s).
- The key variable for outdoor comfort, i.e. mean radiant temperature T_{mrt} , is also calculated.

2.8.2 RAY-MAN

Ray Man includes the Munich Energy Balance Model for Individuals (MEMI). The MEMI model is based on the energy balance equation (2) for the human body (Höppe 1993):

$$M+W+R+C+E_D+E_{RE}+E_{SW}+S=0 \quad (2)$$

M.....metabolic rate (internal energy production)

W.....physical work output

Rnet radiation of the body

Cconvective heat flow

E_D Latent heat flow to evaporate water diffusing through the skin (imperceptible perspiration)

E_{re} sum of heat flows for heating and humidifying the inspired air

E_{SW}heat flow due to evaporation of sweat

Sstorage heat flow for heating or cooling the body mass.

„[...]Furthermore, the positive sign in front of the parameter is applied when there is an energy gain, and the negative when there is an energy loss (M is always positive; W , E_D and E_{sw} are always negative). The unit of all heat flows is in Watt (Höppe 1999). The individual activity of humans (in Watt) and heat flows in equation 2, are controlled by the following meteorological parameters (Verein Deutscher Ingenieure 1998; Höppe 1999):

- *Air temperature: C , E_{Re}*
- *Air humidity: ED , E_{Re} , E_{Sw}*
- *Wind velocity: C , E_{Sw}*
- *Mean radiant temperature: R*

Thermo-physiological parameters are required in addition:

- *Heat resistance of clothing (clo units)*
- *Activity of humans (in Watt) [...].*

Physiological equivalent temperature (PET) can be calculated with the bioclimatic and radiation model RAY-MAN, which is appropriate for calculation of thermal indices such as PET, PMV and SET. This software is free and accessible for public (Matzarakis and Amelung 2008).

3 METHOD

3.1 Overview

The main objective of this study is to identify the most effective mitigation measure, or a combination of few measures, in order to reduce air temperature and increase outdoor thermal comfort in the inner city of Vienna, Austria. The research method for this project is based on simulation.

The meteorological data such as the air temperature, wind speed, relative humidity, and wind direction were collected from AKH weather station, during summer period, from 19.08.2012 to 21.08.2012, in order to conduct simulation with a numerical model (ENVI-MET) for 24-hour cycle. Moreover, the measured data were used for calibrating the simulation tool. The simulation results from each scenario have been compared to find the most effective combined mitigation scenario, in view of reducing air temperature and increasing the outdoor thermal comfort. The results are shown in chapter 4.

3.2 Case study

For the purpose of this project, the street called Herbstrasse in a metropolitan area in Vienna in 16th district has been selected (Figure 24). It was selected based on the availability of the weather data previously collected on-site, and as it was found adequate to conduct envisioned mitigation scenarios. Table 5 provides an overview of the main properties of Herbstrasse:



Figure 24: Herbstrasse, (<http://www.wien.gv.at/stadtplan/> and Google map 2014)

Table 5: The properties of the Herbsstrasse

Property	Non-vegetated canyon
Orientation	SE / NW
Street width [m]	18
Building height [m]	16 - 20
Building materials	Plastered bricks
Paving material	Black asphalt, cement concrete
Vegetation	None
Mean SVF [%]	45
Traffic level	Low

3.3 Weather data

The required input meteorological data used to run simulations with the aid of the ENVI-MET tool for each day are: air temperature, relative humidity, wind speed, and wind direction. The simulations were run for the time period of minimum of 6 hours and maximum of 24 hours. The data which were collected with a mobile weather station in Herbsstrasse were collected at the specific time of the day only (during mornings and afternoons), thus were not complete to represent the 24-hour cycle. Therefore, the data of AKH weather station have also been used for this project. AKH weather station is close to the Herbsstrasse (as seen in Figure 25). In addition, the measured data were used for calibrating the simulation tool.

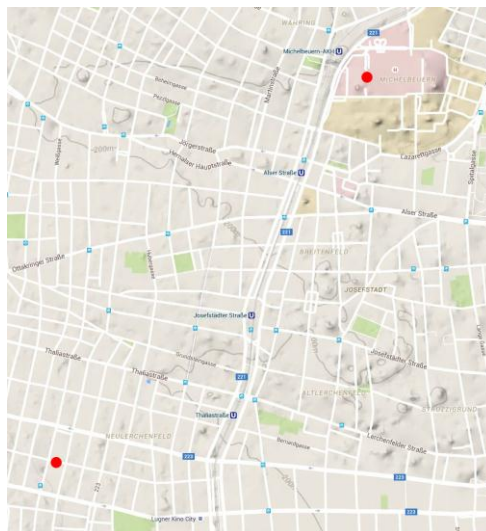


Figure 25: The position of AKH weather station relative to Herbsstrasse (Google Maps 2014)

Model area

3.3.1 ENVI-MET

The model area has a size of about 365*175 m, resulting in 73*35*30 cells with a resolution of 2.00*2.00*2.00 meters, and the size of the grid is 5*5 meters. Note that, the resolution 2.10*2.10*2.10 is used for first, second, and third scenarios, on 21.08.2102 in order to reduce the possible errors during the process. The geographic coordinates of the model area were set to 48.13° northern latitude and 16.22° eastern longitude. Also, the plan (Figure 26) shows the position of three receptors within the street. The height of the sensor is set on 1.4 meters above the ground, as this is the recommended height when assessing the outdoor human thermal comfort (Gartland 2008).

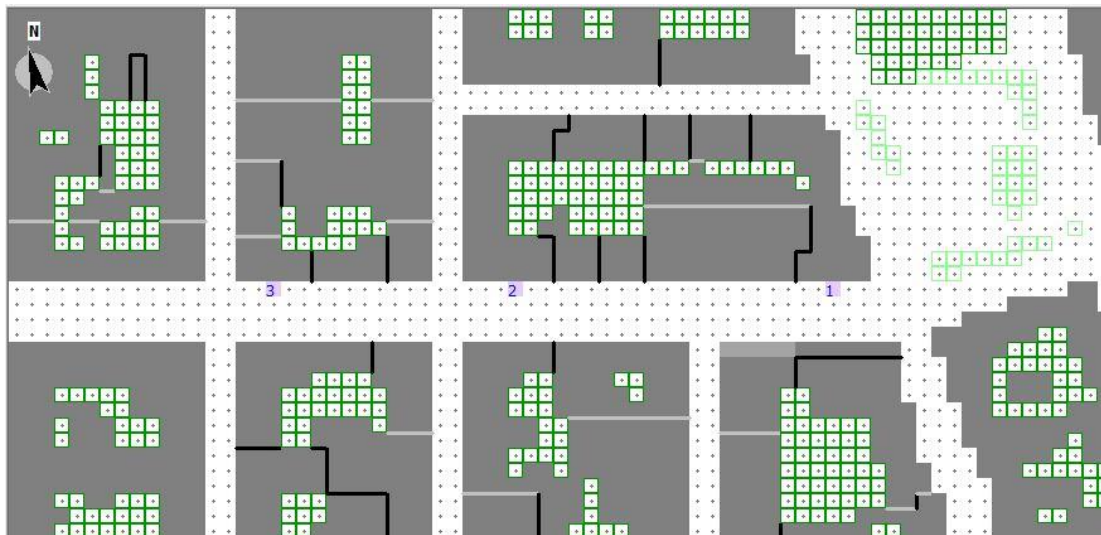


Figure 26: The model area as seen in ENVI-MET and the position of receptors on the street

Before running the simulation, and in order to allow for the dynamic change of the meteorological background, the values of air temperature and relative humidity were manually predefined within the simulation tool to represent the actual measured conditions at a specific hour. This process is called simple forcing (Figure 27).

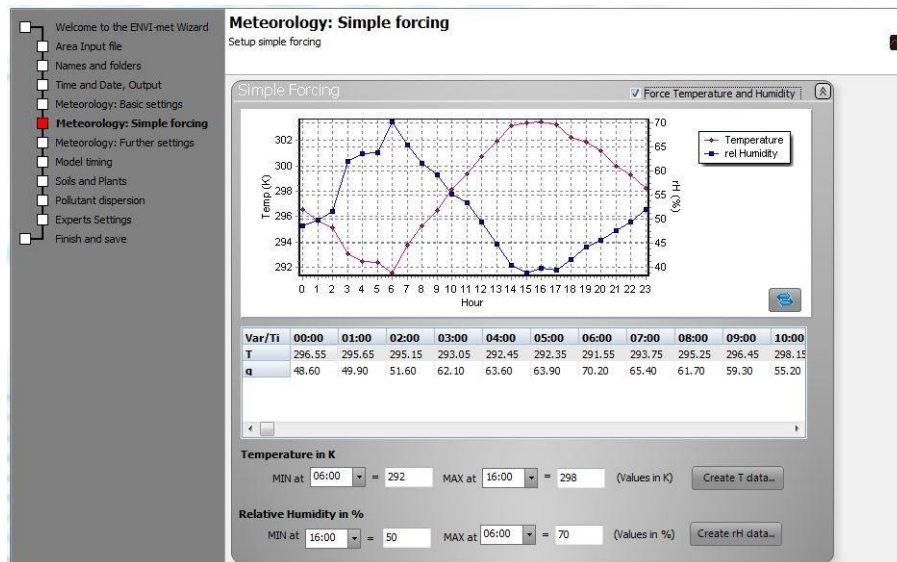


Figure 27: Simple forcing

3.3.2 RAY-MAN

As mentioned earlier, this software is capable to calculate the PET. Making the geometry (Figure 28) and assigning the meteorological data such as the air temperature, wind speed, relative humidity, and mean radian temperature (Figure 29) are important factors for the reliable calculation of PET. According to Matzarakis and Mayer (1999), [...] *Depending on the objectives of the evaluation, these meteorological parameter can be measured experimentally or calculated in a grid-net by numerical models. [...]*

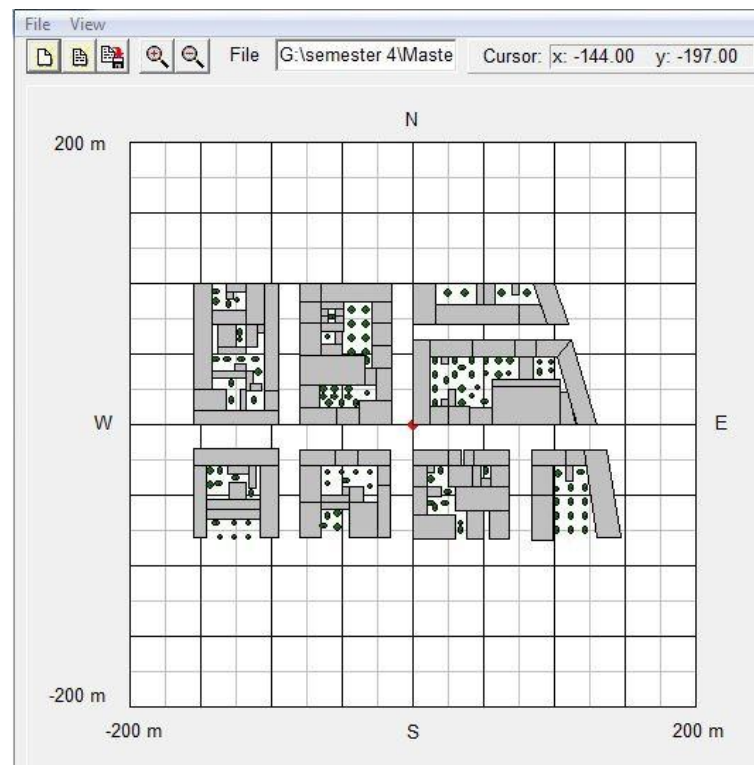


Figure 28: The plan of model in RAY-MAN

Also, the mobile weather stations are not able to record the Mean Radiant Temperature if not properly equipped (Matzarakis and Mayer 1999), thus resulting in unreliable data. Therefore, to avoid possible uncertainties, the value of solar radiation had been used instead of the value of mean radiant temperature in order to calculate the value of PET for the basic model. This was then repeated for all simulation days. The position of sensors used to assess the values of meteorological data is 1.1 meter above the ground (the average height of a standing person's centre of gravity in Europa) (Matzarakis and Mayer 1999).

The screenshot displays the RayMan 1.2 software interface, which is used for calculating thermal comfort indices. The interface is divided into several sections for data input:

- Date and time:** Date (day.month.year) is 20.8.2012, Day of year is 233, and Local time (h:mm) is 21:00. A "Now and today" button is present.
- Geographic data:** Location is set to "ÖSTERREICH". There are buttons for "Add location" and "Remove location". Geographic coordinates are: Geogr. longitude (° ' E) 16°13', Geogr. latitude (° ' N) 48°12', Altitude (m) 323, and time zone (UTC + h) 1.0.
- Current data:** Air temperature T_a (°C) is 20.0, Vapour pressure VP (hPa) is 12.5, Rel. Humidity RH (%) is 53.5, Wind velocity v (m/s) is 1.0, Cloud cover C (octas) is 0, Global radiation G (W/m²) is empty, and Mean radiant temp. T_{mrt} (°C) is empty.
- Personal data:** Height (m) is 1.75, Weight (kg) is 75.0, Age (a) is 35, and Sex is m.
- Clothing and activity:** Clothing (clo) is 0.9 and Activity (W) is 80.0.
- Thermal indices:** There are checkboxes for PMV, PET (which is checked), and SET*.
- Calculation:** A section with "New" and "Add" buttons.

The interface also includes a menu bar (File, Input, Output, Table, Language, ?), a toolbar with standard window controls, and a "Close" button at the bottom right.

Figure 29: Assigned meteorological data

3.4 Hypothesis

For the purpose of this project, it has been assumed that the use of materials with high thermal reflectance and high thermal emittance, and additionally, increasing the vegetation within the area, could lead to reduction of air temperature and increase of outdoor thermal comfort.

3.5 Statistical Analysis

3.5.1 Simulation Input Data

In this project, the data have been divided into two categories:

1. **Data for making the model:** These data include the building height, the street width, the building materials, the paving materials, as well as, the geographic data.
2. **Data for running the simulation:** these data include the meteorological data such as the air temperature, relative humidity, wind speed, and wind direction.

The meteorological data which were provided by B. Dimitrova and M. Vuckovic were not enough to run simulation in ENVI-MET. Therefore, the simulations carried out using meteorological data of AKH weather station.

3.5.2 Simulation Output Data

The objectives of this research are to find effective mitigation scenario in order to reduce the air temperature, and secondly, to increase the outdoor thermal comfort by using the materials with high albedo, high emissivity and vegetation. The necessary meteorological data needed as the input for RAYMAN model has been calculated for all envisioned scenarios by the simulation tool ENVI-MET.

Necessary input data to calculate PET using RAYMAN are:

1. The meteorological data such as the air temperature, relative humidity, wind speed and mean radiant temperature. This software is not able to assign cool roof and cool paving materials to surfaces, thus just the buildings and trees are defined.
2. Geometry data such as the building footprint and representative height are defined.
3. Geographic coordinate such as geographic latitude (...°..'N), geographic longitude (...°..'E), altitude (m), time zone.
4. Thermo-physiological factors, such as activity of humans and clothing.

The meteorological data are calculated by ENVI-MET tool and then the value of each meteorological parameter will be assigned to RAY-MAN model. Generally, the thermo-physiologic parameters are constant in RAYMAN (such as, the human activity and clothing), but it is possible to change them manually. Note that, the RAY-MAN is able to calculate the thermal indices such as SET and PMV.

3.6 Scenarios

As previously mentioned, the research method for this project is based on simulation conducted for three specific summer days (Table 6). Therefore, the meteorological data were collected from weather station, at the same time, in order to conduct the simulation with a numerical model for a 24-hour cycle. Moreover, for each day the basic model (BS) and all three envisioned scenarios (S1, S2, and S3) were simulated.

Table 6: Overview of simulation days and respective scenarios

	Day	Date	Basic model (BS) First Scenario (S1) Second Scenario (S2) Third Scenario (S3)
1	Day 1	19.08.2012	
2	Day 2	20.08.2012	
3	Day 3	21.08.2012	

3.6.1 Basic model (BC)

This model is the base case ('as is' case portraying the realistic state of the area), that is further compared with another scenarios. The material used for pedestrian zone (sidewalks) and street is black asphalt. The height of the buildings is between 15-20 meters and the width of street is 18 meters. Figure 30, and 31 show the plan and perspective of the basic model. The receptors were placed in 3 different spots within the street (as seen in Figure 30).

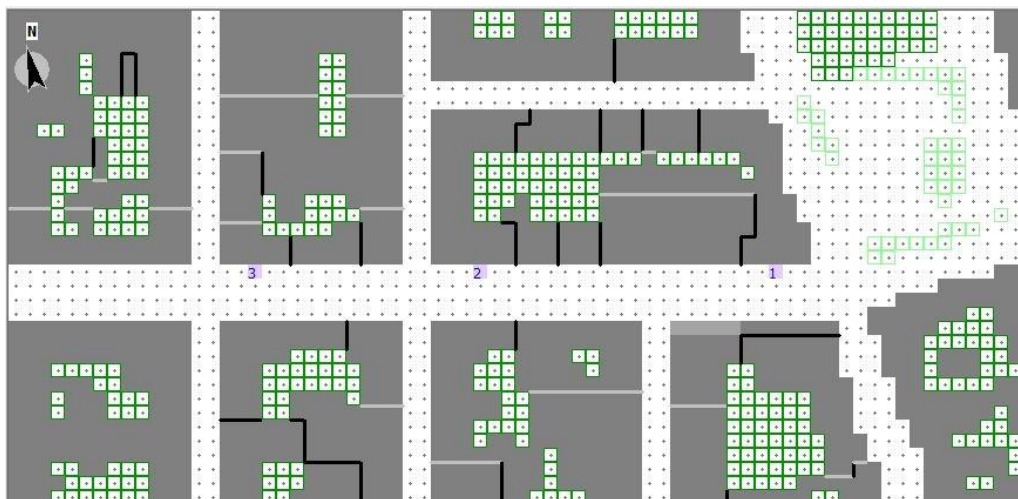


Figure 30: The plan of the basic model

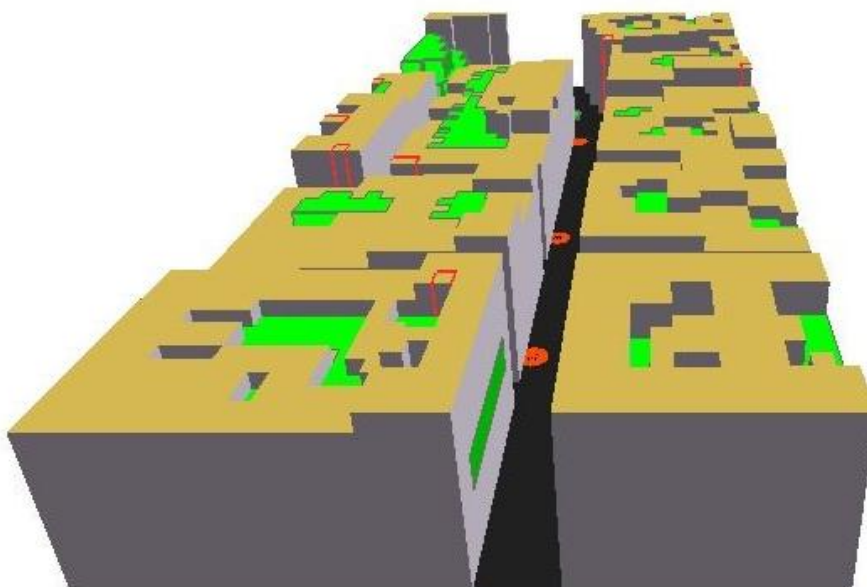


Figure 31: The perspective of the basic model

3.6.2 First scenario (S1)

In the first scenario white roofs and trees have been assigned. Distance between the trees in this scenario is around 20 meters. For the purpose of the present scenario, the trees are placed on one side of the street only, in order to provide the shade for south-faced buildings. Figure 32 and 33 show the plan of first scenario and perspective respectively.

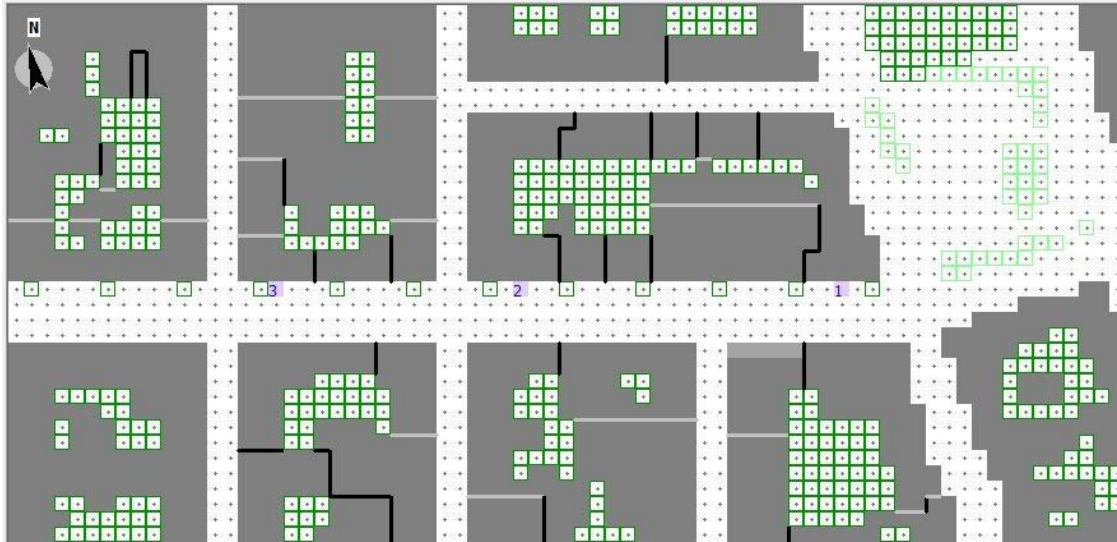


Figure 32: The plan of the First scenario

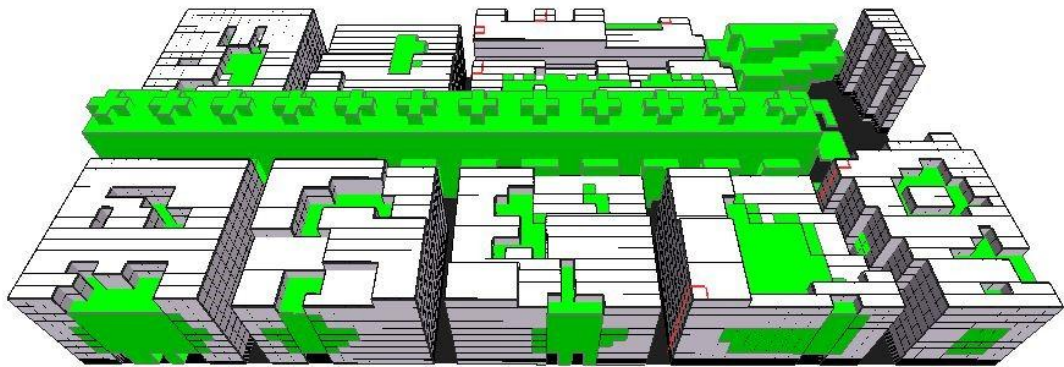


Figure 33: The perspective of the First scenario

3.6.3 Second Scenario (S2)

Mitigation measures in this scenario include light colored concrete for pedestrian way, assigned on both sides of the street, and red road coating for motorway, and additionally, the trees have been assigned close to the south-faced buildings. Moreover, the distance between trees is between 25-30 meters. Figures 34 and 35 show the plan of second scenario and perspective, respectively.

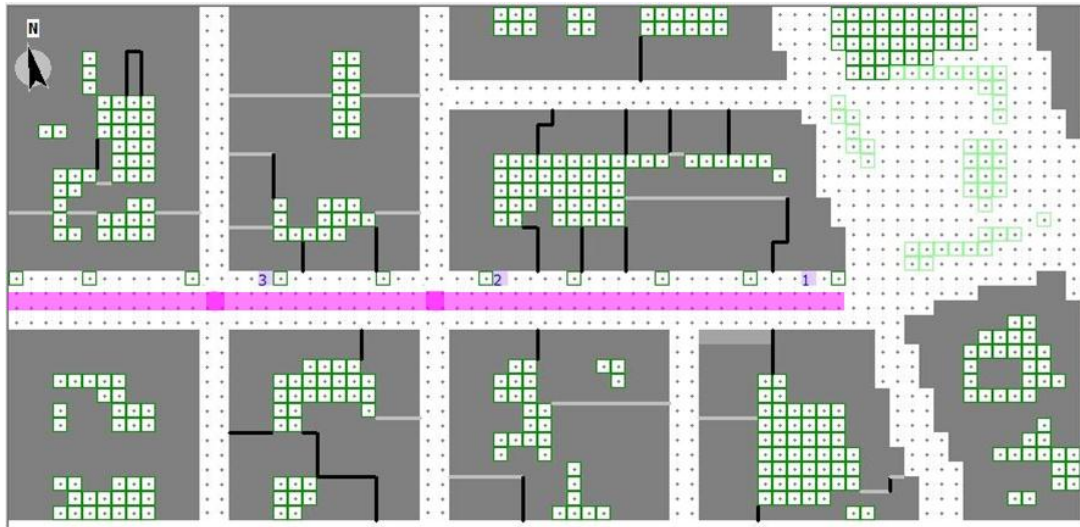


Figure 34: The plan of the second scenario

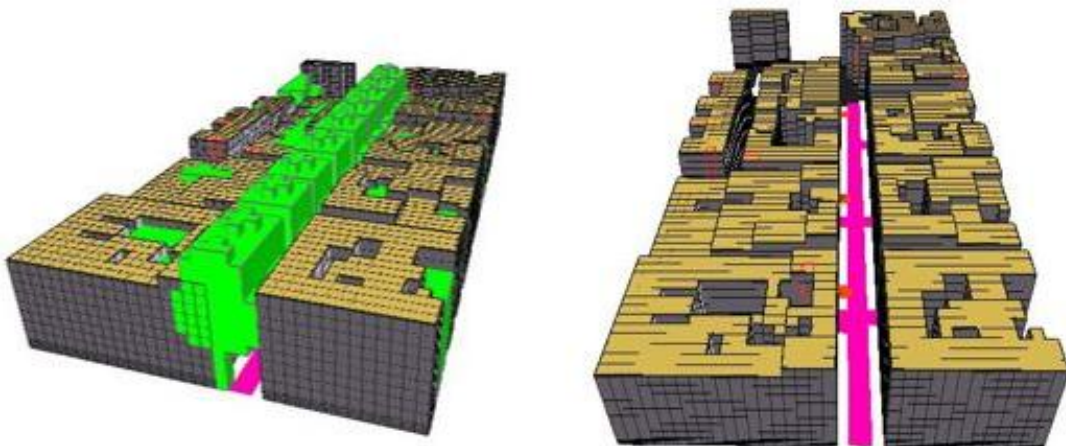


Figure 35: The perspective of the second scenario (the image on the right omits trees and shows the position of applied red coating)

3.6.4 Third scenario (S3)

Mitigation measures in this scenario include light colored concrete for pedestrian way assigned to just one side of the street, black asphalt for motorway, the extensive green roofs, and additionally, the trees that have been assigned on both sides of the street. Figures 36 and 37 show the plan of the third scenario and perspective.

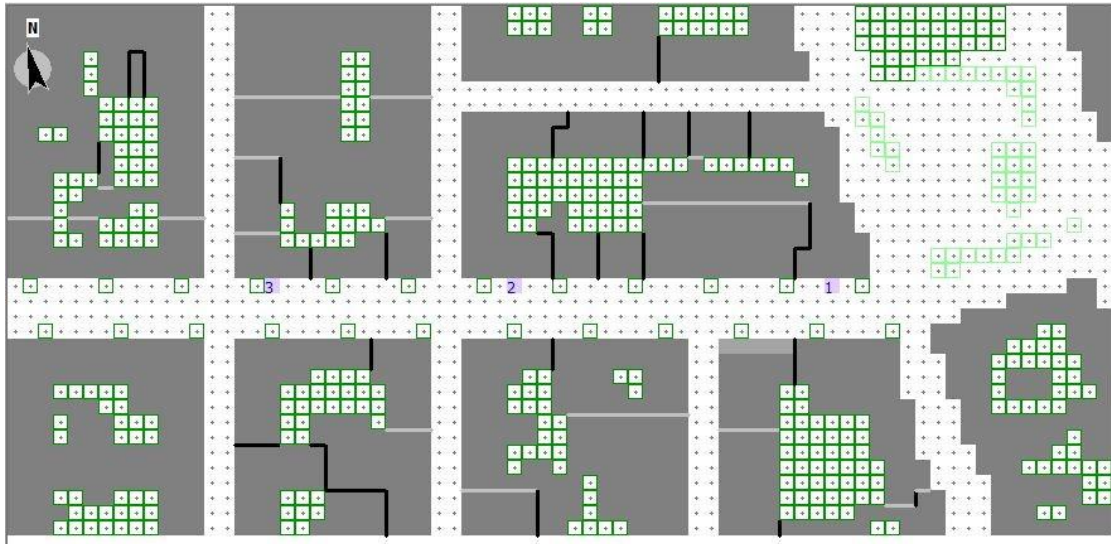


Figure 36: The plan of the third scenario

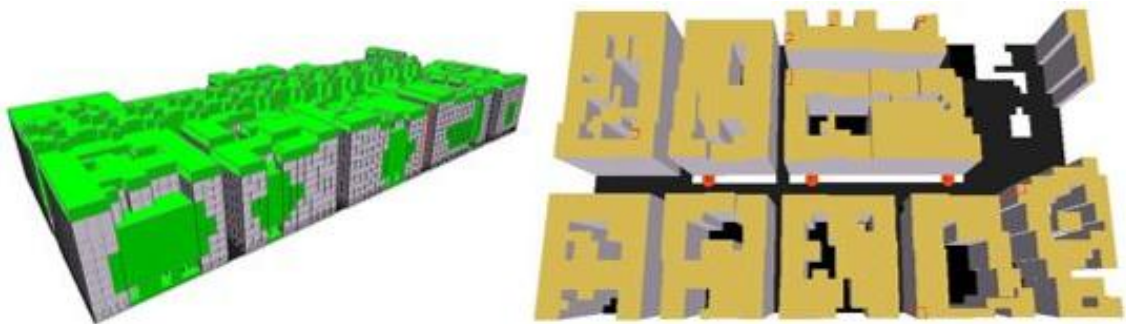


Figure 37: The perspective of the third scenario

4 RESULTS

4.1 Overview

This chapter will provide an overview of the main simulation results. This chapter will focus on analysing the air temperature and the Physiological Equivalent Temperature (PET) resulting from each scenario. Simulations have been carried out during the summer period, more precisely on 19.08.2012 and 20.08.2012, for 24-hour cycle and with one-hour interval. Further results (illustrating the conditions of 21.08.2012) can be found in the appendix.

4.1.1 DAY 1

Basic model (Without Mitigation)

This scenario consisted of buildings with plastered walls, tiled roofs and asphalt for pedestrian and street area. Therefore, this simulation was conducted in order to find the appropriate base reference model. The simulation results were then compared to the measured data to assess the degree of the agreement (Figure 38). Firstly, when compared to the actual data (purple dots in the figure), the difference was found not to be significant, and the model was deemed acceptable for the ongoing analysis. Secondly, the results clearly demonstrate that there is no significant difference of the main climatic parameters between three receptors (R1, R2, and R3). When the sampling is done on a small area, the gradients are often negligible (Oke 2005).

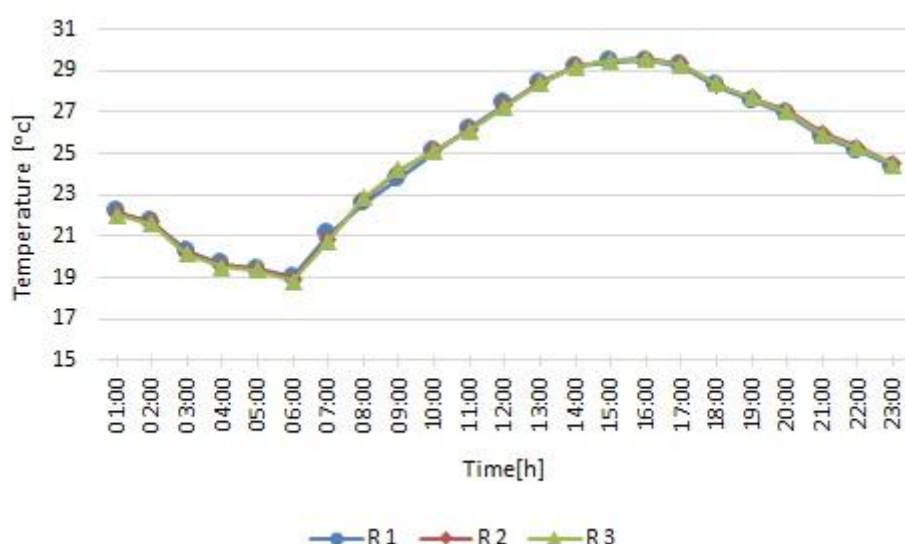


Figure 38: Simulated air temperature of BC Model on 19.08.2012

Figure 39 shows the average air temperature sampled from the three receptors, for all four models. The results show that the effects of combined mitigation strategies result in slight air temperature reduction when compared to the basic model. This is further seen in all scenarios. However, the highest offset is observed during the morning and late afternoon hours. This reduction can be as high as 0.6 K.

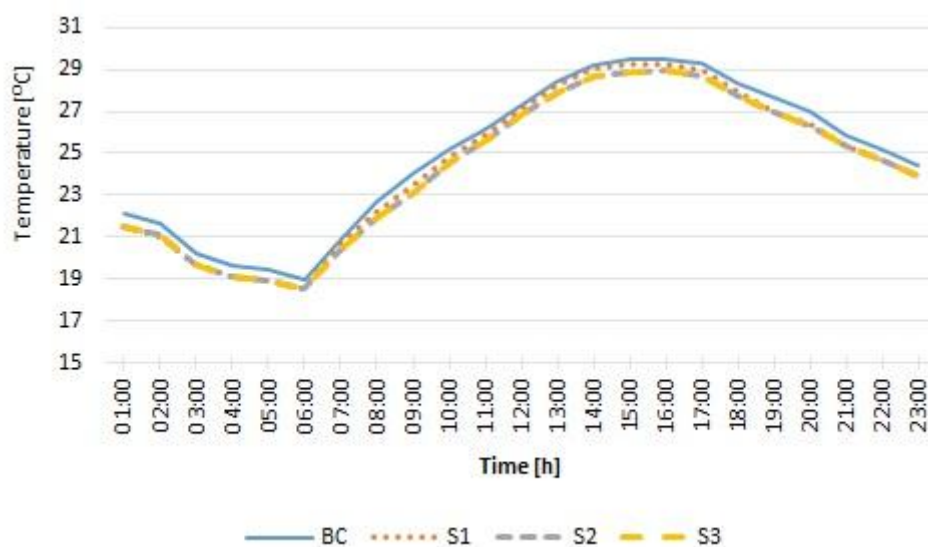


Figure 39: Simulated average air temperature on 19.08.2012

Physiological Equivalent Temperature

Figure 40 shows the distribution of PET for each receptor of the basic model. It can be clearly seen that the difference of PET for the receptor 1 is larger than the receptors 2 and 3. Furthermore, there is a peak for all three receptors noted during early morning hours. This might be explained in relation to the geometry, as the overall solar gain was higher during morning hours, due to the fact that all three receptors were directly exposed to incoming solar radiation at this time. To further elaborate on this point, consider Figure 41 which shows the 24-hour distribution of Mean Radiant Temperature (T_{mrt}) for all three receptors for BC. It can be seen that all three receptors measured higher T_{mrt} during early morning hours, more specifically starting from 06:00 for R1, and around 08:00 for R2 and R3. As mentioned previously, this might be attributed to the direct exposure to the incoming solar radiation.

However, these differences are smaller when the mitigation scenarios S1, S2 and S3 are applied (as seen in Figures 42 to 44), but still existing. Again, this may be attributed to the geometry and shading effect of trees considered in respective scenarios.

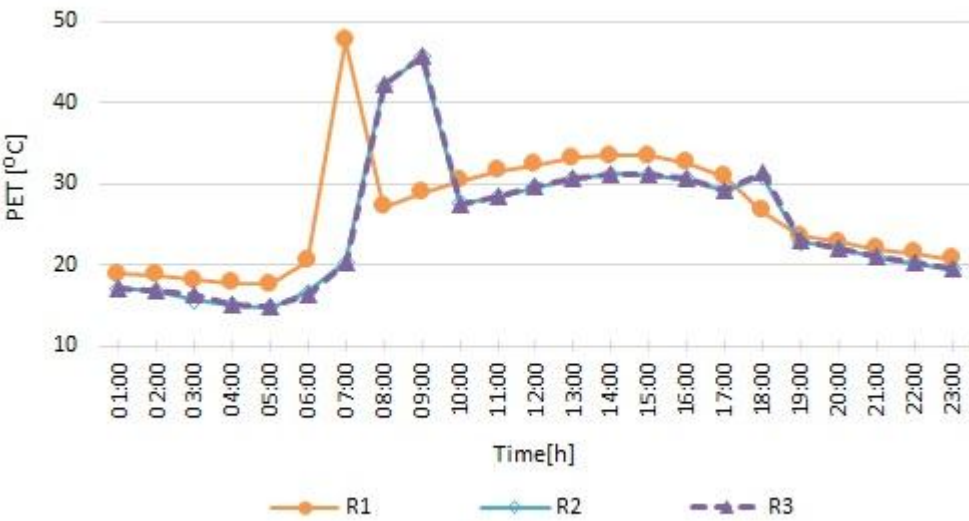


Figure 40: Physiological equivalent temperature of the BC on 19.08.2012

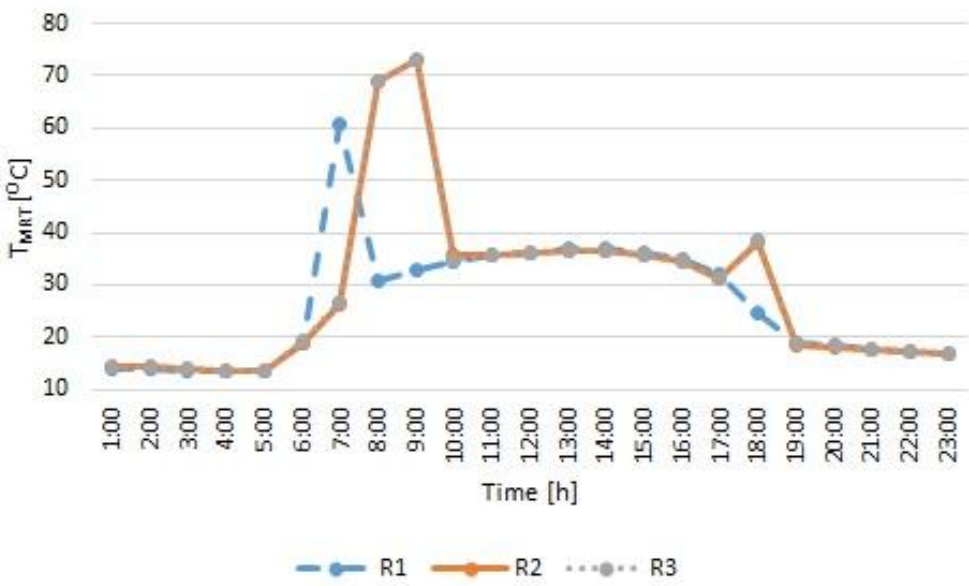


Figure 41: Mean Radiant Temperature of the BC on 19.08.2012

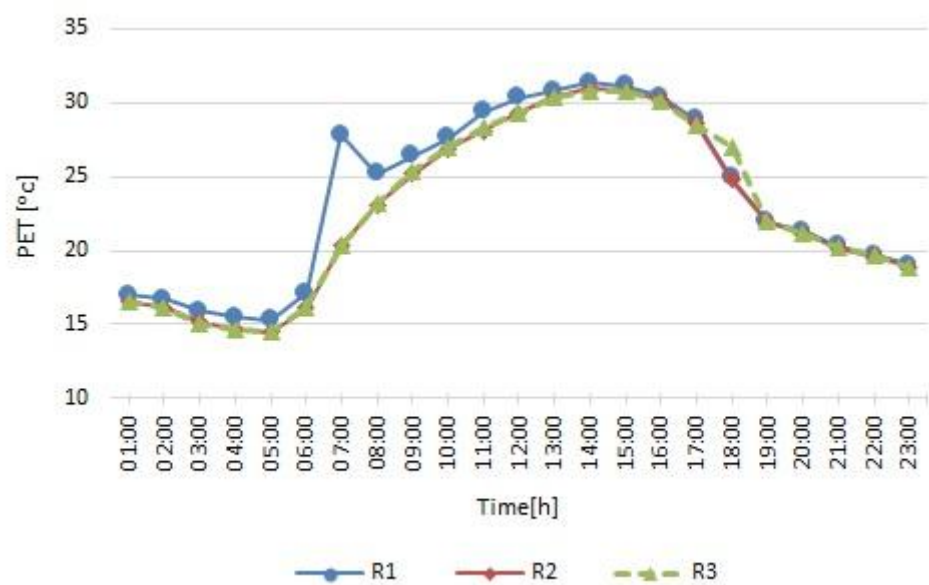


Figure 42: Physiological equivalent temperature of the S1 on 19.08.2012

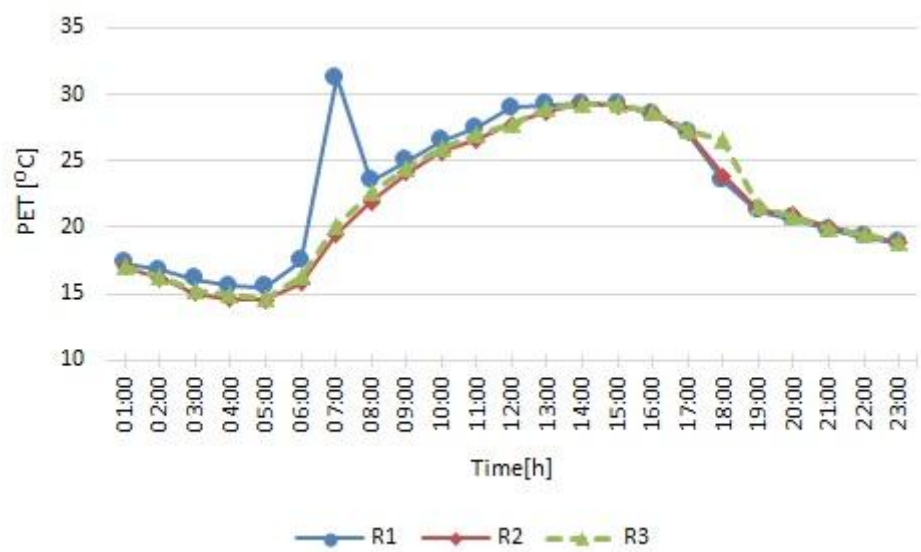


Figure 43: Physiological equivalent temperature of the S2 on 19.08.2012

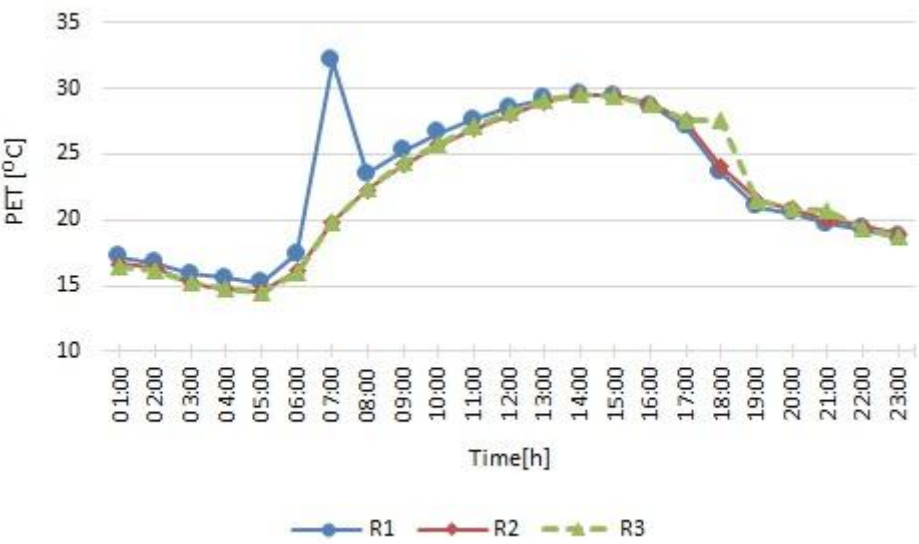


Figure 44: Physiological equivalent temperature of the S3 on 19.08.2012

4.1.2 DAY 2

Basic models (Without Mitigation)

This scenario consisted of buildings with plastered walls, tiled roofs and asphalt for pedestrian and street area. The purpose of this model was to assess the most appropriate base model to run the envisioned mitigation scenarios. Once the simulation data was compared to the measured one (Figure 45), a significant difference was not apparent. Therefore, the model was deemed acceptable for the ongoing study.

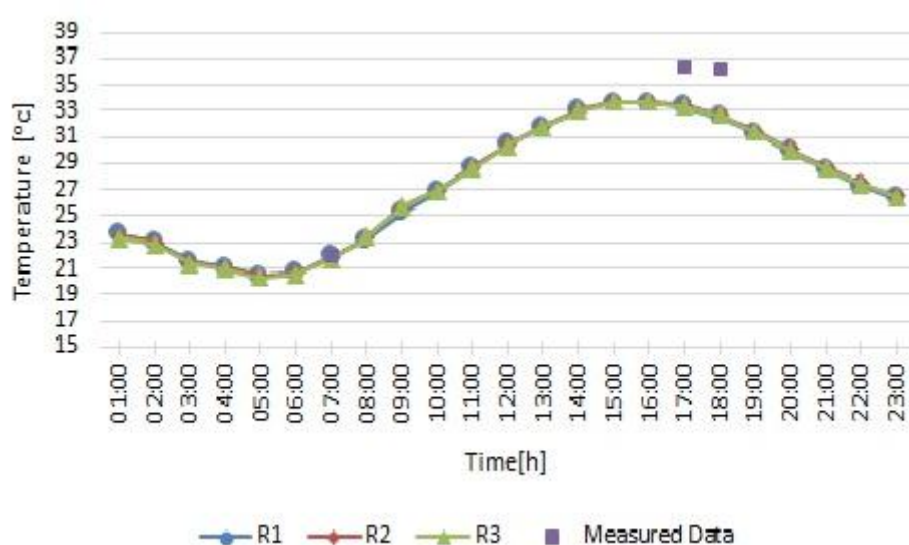


Figure 45: Simulated air temperature of BC on 20.08.2012

Figure 46 shows the average air temperature sampled from the three receptors for four models. The results show that the effects of combined mitigation strategies result in slight air temperature reduction when compared to the basic model. This is further seen in all scenarios. However, the highest offset is observed during the late afternoon hours and nighttime.

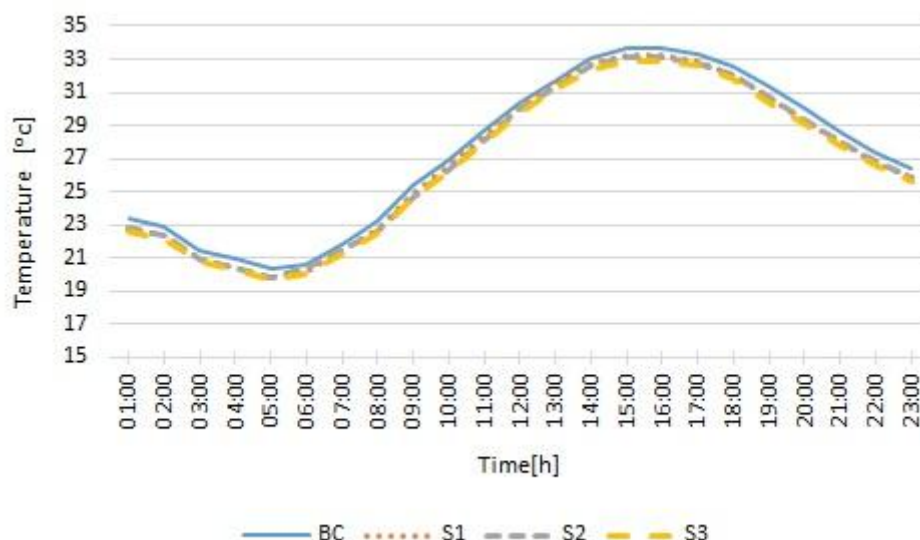


Figure 46: Simulated average air temperature on 20.08.2012

Physiological Equivalent Temperature

Figure 47 shows the PET for each receptor of the basic model. It can be clearly seen that the difference of PET of the receptor 1 is larger than the receptors 2 and 3. As noted in the previous day, during early morning hours considerable higher PET was measured for all three receptors, which again may be attributed to the specific geometry and higher exposure to the incoming solar radiation (as seen from T_{mrt} values in Figure 48).

However, these differences are smaller when the mitigation scenarios S1, S2 and S3 are applied (as seen in Figures 49 to 51). Furthermore, the effects on the outdoor thermal comfort are found to be higher. Again, due to the shading effect of trees implemented in respective scenarios, and due to the higher solar exposure of R1, PET was considerably higher for R1 during the early morning hours.

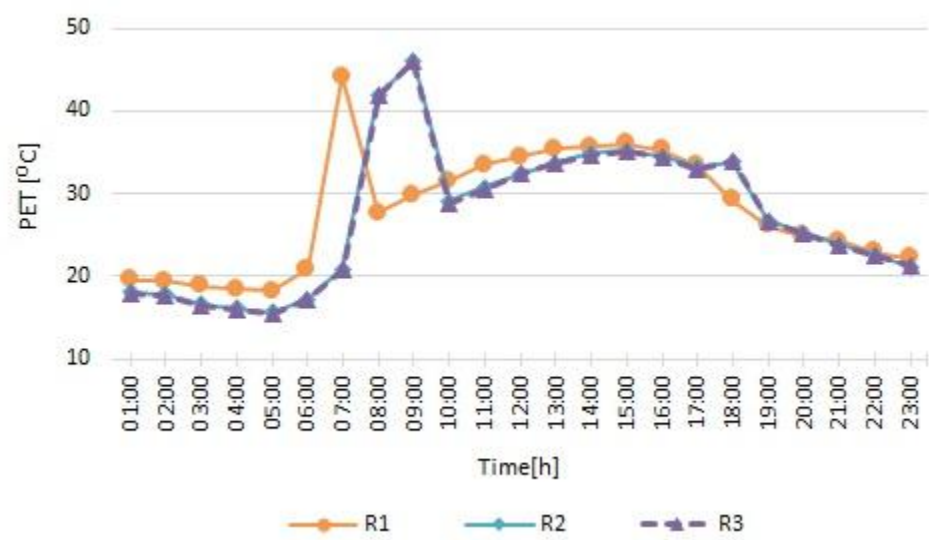


Figure 47: Physiological equivalent temperature of the BC on 20.08.2012

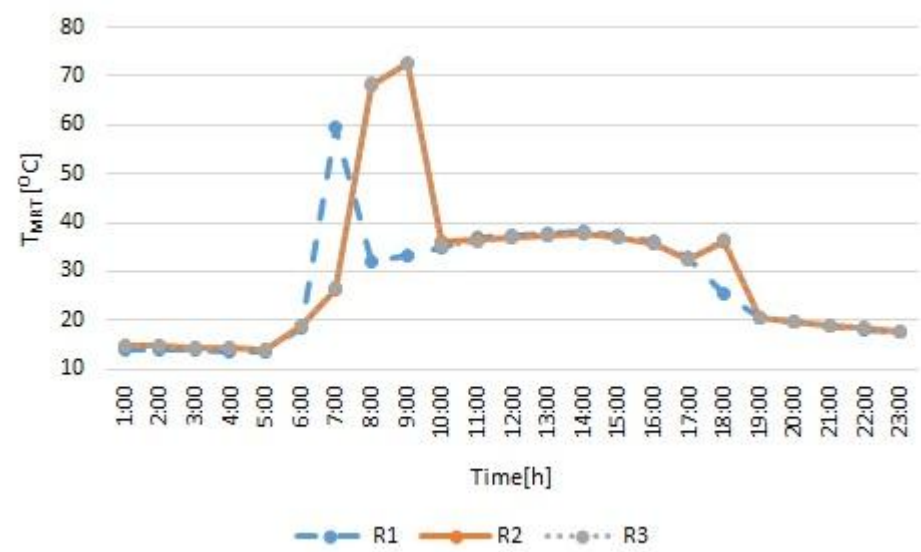


Figure 48: Mean Radiant Temperature of the BC on 20.08.2012

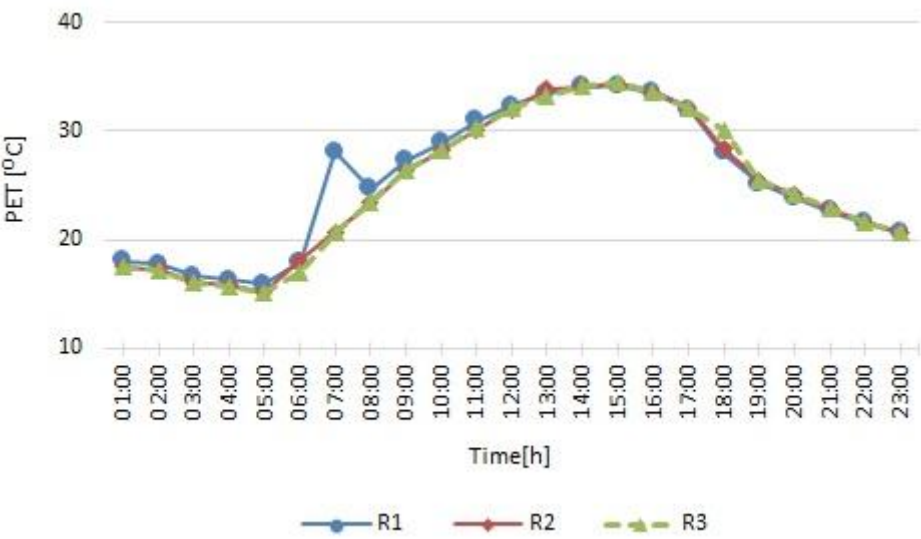


Figure 49: Physiological equivalent temperature of the S1 on 20.08.2012

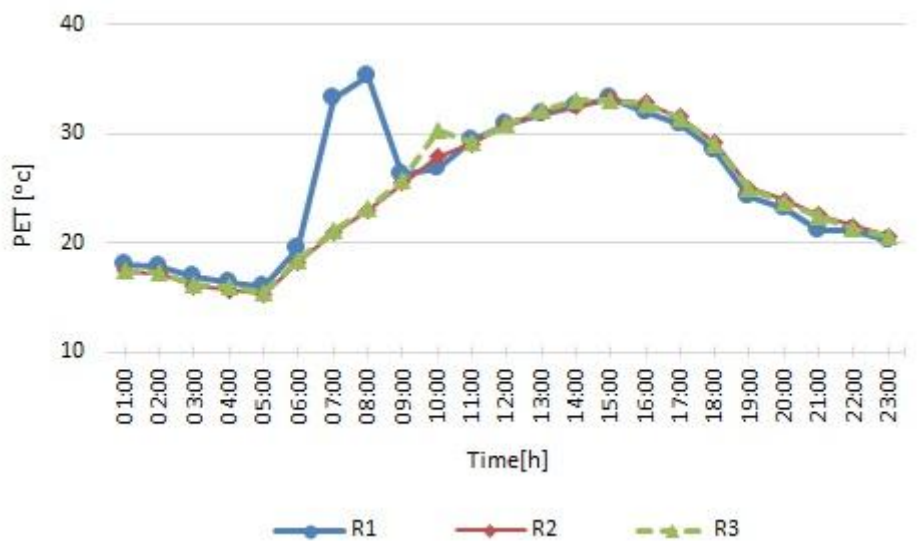


Figure 50: Physiological equivalent temperature of the S2 on 20.08.2012

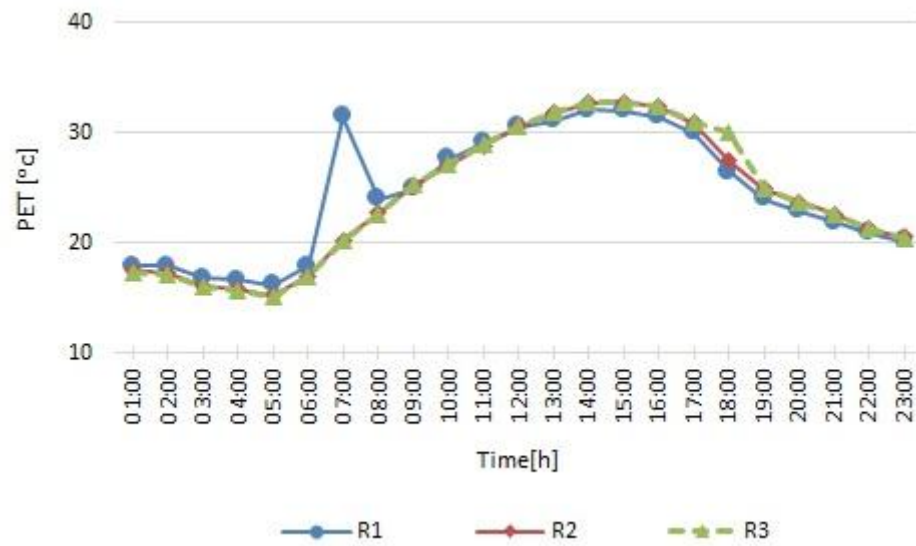


Figure 51: Physiological equivalent temperature of the S3 on 20.08.2012

5 DISCUSSION

5.1 Overview

As it can be seen from the results, the envisioned mitigation scenarios display slight improvement on the air temperature when observed on the micro-scale. However, the reduction in view of the PET index is more significant. This improvement is further noted in each of the proposed scenarios. In general, it can be said that, when a number of urban interventions are applied together, the effect in terms of the overall reduction in both air temperature and PET is most favorable.

5.2 Day 1

5.2.1 Average difference of air temperature between BC and S1-S2-S3

Figure 52 shows the difference in air temperature between BC and three scenarios (S1, S2, and S3) on 19.08.2012. It can be observed that S2 and S3 resulted in approximately equal reduction of air temperature, however, displayed in different time. The cooling effect of S2 was more pronounced during the daytime, while the S3 was proven more effective during the nighttime. Scenario 2 shows the greatest daytime reduction of air temperature, in range of 0.5K to 0.9K.

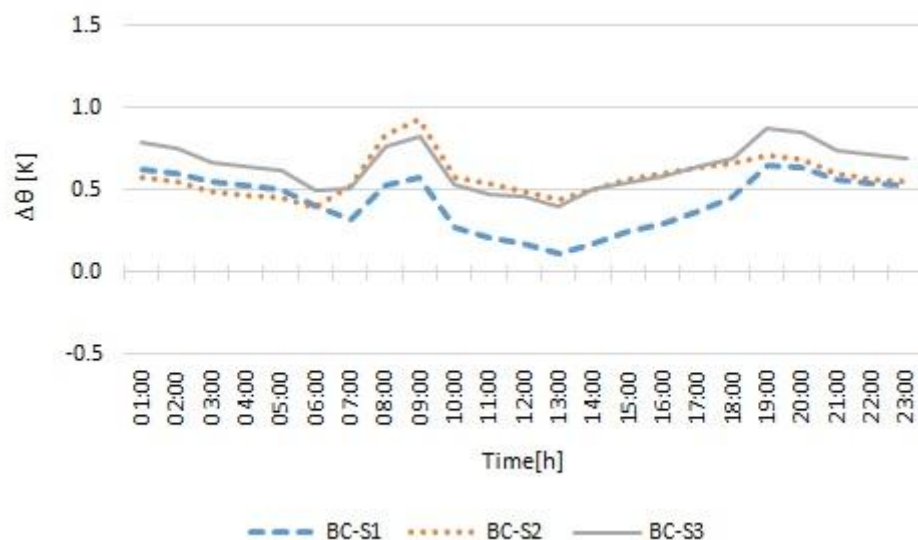


Figure 52: Average air temperature difference between BC and S1-S2-S3 on 19.08.2012

The peak reduction was noted during the early morning hours, but lasting only for 3 hours. Scenario 3 shows that the air temperature reduction achieved was about 0.8 K. However, even if the peak reduction was smaller than that noted in Scenario 2, the time frame was longer, lasting around 10 hours. In general, Scenario 1 was proven to be the least effective of all interventions analyzed, and especially during the daytime. During the nighttime, the mitigation effect was noticeably improved. It can be further concluded that the Scenario 3 proved to be the most beneficial.

5.2.1 Compared PET between BC and S1, S2 and S3

Figure 53 shows the output PET values collected at one receptor (R3) for all four models (BC, S1, S2, and S3). In general, it can be observed that the most pronounced PET reduction was during the early morning (from 06:00 until 10:00) and late afternoon hours (from 17:00 until 19:00). This circumstance might be due to the overall higher solar gain noted in this particular time, resulting in increased mean radiant temperature of the Base Case. However, during the daytime, the PET of Base Case decreased dramatically, which might be due to the sudden cloud cover forming over the area. During the remaining hours, the PET curve resulting from envisioned scenarios followed the one from the Base Case. However, it can be said that S2 and S3 performed better than Scenario 1, resulting in an offset of around 2K between the respective lines. Additionally, this circumstance was more pronounced during the daytime, when the average reduction was found to be the greatest.

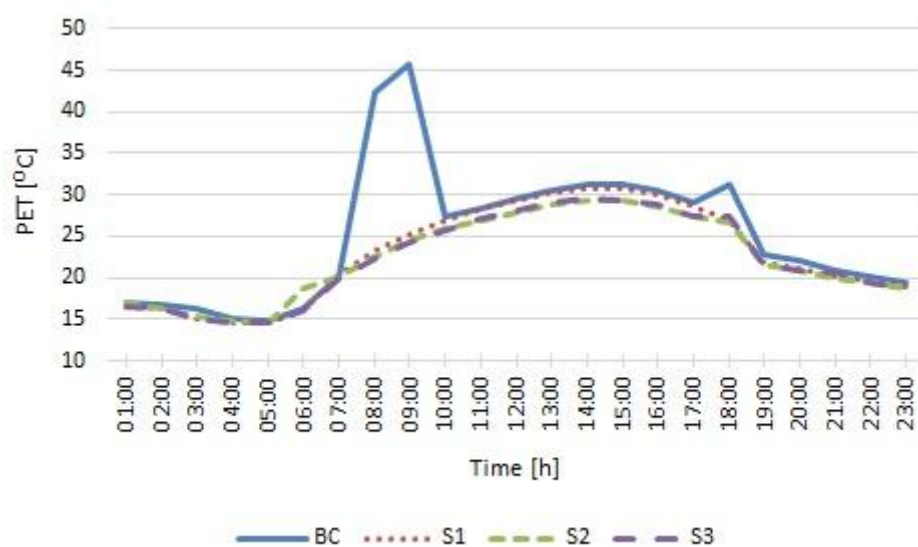


Figure 53: Compared the average PET between four Models on 19.08.2012 at R3

Table 7 shows the average difference of PET values collected from three receptors of basic models and three scenarios, respectively. As it can be seen from the table, the average PET between BC-S1 is 2.54 K and between BC-S2 and BC-S3 is 3.21 K and 3.15 K. Therefore, Scenario 2 was proven to be the most effective in terms of the improved outdoor thermal comfort, whereas Scenario 3 displayed the highest reduction of air temperature.

Table 7: Average difference PET and air temperature on three receptors on 19.08.2012

Date	Scenario	ΔPET [K]			ΔT [K]		
		R1	R2	R3	R1	R2	R3
19.08.2012	BC-S1	2.89	2.41	2.33	0.52	0.4	0.37
	BC-S2	3.57	3.17	2.89	0.62	0.55	0.58
	BC-S3	3.56	3.03	2.86	0.78	0.58	0.58

5.3 Day 2

5.3.1 Average Difference of air temperature between BC and S1-S2-S3

The figure 54 shows the difference in air temperature between BC and three scenarios (S1, S2, and S3) on 20.08.2012. It can be seen that the averaged results of scenario 2 and 3 are approximately equal in reduction of air temperature in different time (same first days). The cooling effect of scenario 3 was more pronounced during day and night than scenario 2. The scenario 3 shows the greatest nighttime reduction of air temperature, in range 0.7K to 1K. The peak reduction was noted during the early morning hours and sunset time. Scenario 3 shows that the air temperature reduction achieved was about 1 K. In general, Scenario 1 was proven to be the least effective of all interventions analyzed, and especially during the daytime. During the nighttime, the mitigation effect was noticeably improved. During the nighttime, the mitigation effect was noticeably improved. It can be further concluded that the Scenario 3 proved to be the most beneficial.

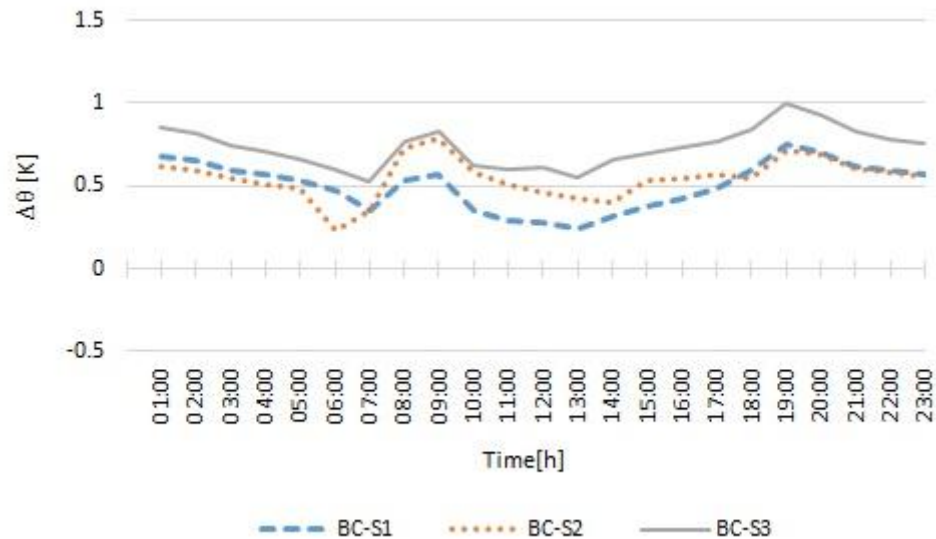


Figure 54: Average air temperature difference between BC and S1-S2-S3 on 20.08.2012

5.3.2 Compared PET between BC and S1, S2 and S3

Figure 55 shows the output PET values collected at one receptor (R3) for all four models (BC, S1, S2, and S3). In general, it can be observed that the most pronounced PET reduction was during the early morning (from 06:00 until 10:00) and late afternoon hours (from 17:00 until 19:00). This circumstance might be due to the overall higher solar gain noted in this particular time, resulting in increased mean radiant temperature of the Base Case. However, during the daytime, the PET of Base Case decreased dramatically, which might be due to the sudden cloud cover forming over the area. During the remaining hours, the PET curve resulting from envisioned scenarios followed the one from the Base Case. However, it can be said that Scenarios 2 and 3 performed better than Scenario 1, resulting in an offset of around 2K between the respective lines. Additionally, this circumstance was more pronounced during the daytime, when the average reduction was found to be the greatest.

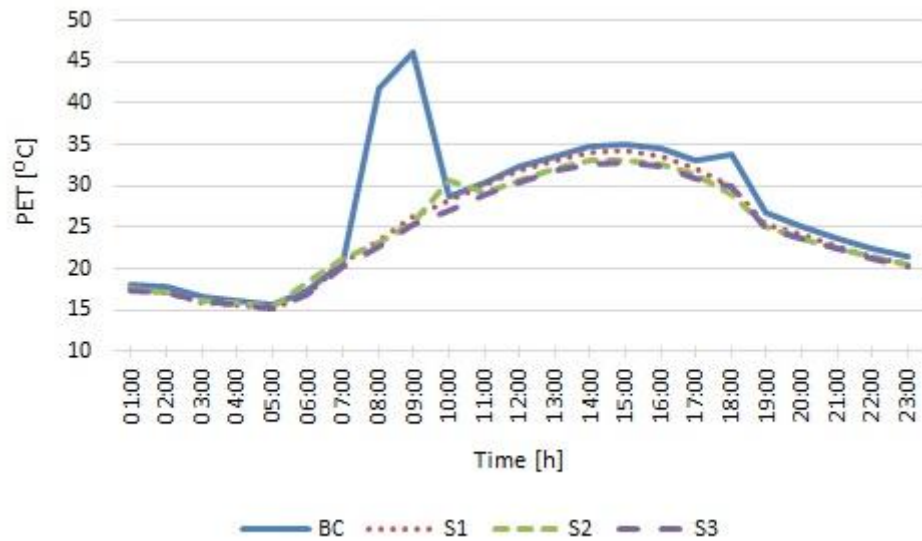


Figure 55: Compared the average PET between four Models on 20.08.2012 at R3

Table 8 shows the average difference of PET values collected from three receptors of basic models and three scenarios, respectively. As it can be seen from the table, the average PET between BC-S1 is 2.46 K and between BC-S2 and BC-S3 is 2.63 K and 3.20 K. Therefore, Scenario 3 was proven to be the most effective in terms of the improved outdoor thermal comfort and the highest reduction of air temperature.

Table 8: Average difference PET and air temperature on three receptors on 20.08.2012

Date	Scenarios	Δ PET [K]			Δ T [K]		
		R1	R2	R3	R1	R2	R3
20.08.2012	BC-S1	2.55	2.45	2.38	0.58	0.48	0.45
	BC-S2	2.43	2.87	2.61	0.55	0.53	0.56
	BC-S3	3.40	3.19	3.03	0.87	0.67	0.67

In summary, finding the most interesting in relation to mitigations that, each of scenarios has significant impact on reduction air temperature and increasing outdoor thermal comfort. However, impact of using the permeable element such as trees has more significant impact on reduction air temperature, increasing outdoor thermal comfort and reduction mean radiant temperature than materials with high albedo and high emissivity.

6 CONCLUSION

This thesis investigates the impact of a number of mitigation scenarios in regard to the air temperature and PET reduction on a sample area in the city of Vienna, Austria. More specifically, the envisioned mitigation scenarios considered implementation of cool roofs, cool pavements, and addition of trees within the urban canyon. The possible reduction of extreme summertime conditions was assessed via numerical microclimate simulation tool.

The results illustrated that the envisioned mitigation scenarios display slight improvement on the air temperature when observed on the micro-scale. The maximum reduction achieved was around 1 K. Furthermore, the results revealed that overall reduction was higher when a combination of few mitigation measures was considered (e.g. trees, increased surface albedo, and green roofs combined).

However, the reduction in view of the PET index was found to be more significant. This might be due to the implementation of trees in each envisioned scenario, and resulting shading effect of vegetation.

Future research

This thesis provided some initial findings on the possible benefits of mitigation measures when ameliorating summertime extremes (e.g. air temperature). As the results look promising, future efforts in this direction are encouraged. Firstly, more detailed datasets are needed, that can provide a 24-hour distribution of essential climatic parameters. Secondly, it would be beneficial to explore a number of additional urban typologies, and assess how these specific measures might perform in different surroundings. Thirdly, it would be interesting to expand the presented study on wintertime, and assess the thermal behaviour of these envisioned scenarios during cold months.

7 INDEX

7.1 List of Figures

Figure 1: Variations of surface and Atmospheric Temperature (Munn 2001).	2
Figure 2: Modification by PBL by cities (Baely 1997)	5
Figure 3: Diagram of the urban Heat Island (Image courtesy of Heat Island Group, Lawrence Berkeley National Laboratory)	6
Figure 4: The diagram of intensity of UHI (Oke 1982)	7
Figure 5: The effect of solar emittance and solar reflectance on roof temperatures (Gartland 2008)	9
Figure 6: Spectrum of solar radiation (EPA 2008).....	9
Figure 7: Comparing white roof and traditional roof (Image courtesy of Heat Island Group, Lawrence Berkeley National Laboratory)	10
Figure 8: Two different type of installation of white roof	11
Figure 9: The different type of Green Roofs (Green business watch 2013)	12
Figure 10: Extensive Green roof (SAFEGUARD 2012)	13
Figure 11: The properties of Grass (Bruse 1999)	13
Figure 12: Compared cool pavement and dark pavement (Image courtesy of Heat Island Group, Lawrence Berkeley National Laboratory)	15
Figure 13: porous pavement (Haus and Wohnen 2011).....	15
Figure 14: Cool paving (BerkeleyLAB)	16
Figure 15: Properties of cool paving (Bruse 1999).....	16
Figure 16: Red road coating (Fietsberaad crow 2011).....	17
Figure 17: The properties of asphalt road with red coating (Bruse 1999).....	17
Figure 18: The properties of regular asphalt (Bruse 1999).....	18
Figure 19: Evapotranspiration (Garden Punk 2012)	19
Figure 20: Two types of deciduous trees	20
Figure 21: Type of coniferous (NukeCZ 2010).....	21
Figure 22: Properties of conifer trees (Bruse 1999)	21
Figure 23: Properties of deciduous trees (Bruse 1999)	21
Figure 24: Herbsstrasse, (http://www.wien.gv.at/stadtplan/ and Google map 2014)	30
Figure 25: The position of AKH weather station relative to Herbsstrasse (Google Maps 2014)	31
Figure 26: The model area as seen in ENVI-MET and the position of receptors on the street	32

Figure 27: Simple forcing	33
Figure 28: The plan of model in RAY-MAN	33
Figure 29: Assigned meteorological data.....	34
Figure 30: The plan of the basic model.....	37
Figure 31: The perspective of the basic model.....	37
Figure 32: The plan of the First scenario	38
Figure 33: The perspective of the First scenario.....	38
Figure 34: The plan of the second scenario	39
Figure 35: The perspective of the second scenario (the image on the right omits trees and shows the position of applied red coating)	39
Figure 36: The plan of the third scenario.....	40
Figure 37: The perspective of the third scenario.....	40
Figure 38: Simulated air temperature of BC Model on 19.08.2012	41
Figure 39: Simulated average air temperature on 19.08.2012.....	42
Figure 40: Physiological equivalent temperature of the BC on 19.08.2012	43
Figure 41: Mean Radiant Temperature of the BC on 19.08.2012.....	43
Figure 42: Physiological equivalent temperature of the S1 on 19.08.2012	44
Figure 43: Physiological equivalent temperature of the S2 on 19.08.2012	44
Figure 44: Physiological equivalent temperature of the S3 on 19.08.2012	45
Figure 45: Simulated air temperature of BC on 20.08.2012	46
Figure 46: Simulated average air temperature on 20.08.2012.....	47
Figure 47: Physiological equivalent temperature of the BC on 20.08.2012	48
Figure 48: Mean Radiant Temperature of the BC on 20.08.2012.....	48
Figure 49: Physiological equivalent temperature of the S1 on 20.08.2012	49
Figure 50: Physiological equivalent temperature of the S2 on 20.08.2012	49
Figure 51: Physiological equivalent temperature of the S3 on 20.08.2012	50
Figure 52: Average air temperature difference between BC and S1-S2-S3 on 19.08.2012....	51
Figure 53: Compared the average PET between four Models on 19.08.2012 at R3	52
Figure 54: Average air temperature difference between BC and S1-S2-S3 on 20.08.2012....	54
Figure 55: Compared the average PET between four Models on 20.08.2012 at R3	55
Figure 56: Simulated air temperature of BC Model on 21.08.2012	69
Figure 57: Simulated average air temperature on 21.08.2012.....	70
Figure 58: Physiological equivalent temperature of the BC on 21.08.2012	71
Figure 59: Mean Radiant Temperature of the BC on 21.08.2012.....	71
Figure 60: Physiological equivalent temperature of the S1 on 21.08.2012	72

Figure 61: Physiological equivalent temperature of the S2 on 21.08.2012	72
Figure 62: Physiological equivalent temperature of the S3 on 21.08.2012	73
Figure 63: Average differenced air temperature between BC and S1-S2-S3 on 21.08.2012 .	74
Figure 64: Compared the average PET between four Models on 21.08.2012 at R3	75

7.2 List of Tables

Table 1: The type of Green roofs and their properties as briefly.	12
Table 2: The impact of each mitigation and expected results prior to simulation.....	22
Table 3: Scaled thermal comfort indices for indoor and outdoor (Fanger 1970, Givoni 1976 , ASHRAE 2001 and Toudert 2005)	24
Table 4: Range of PMV and PET for different grade of thermal perception and physiological stress (Matzarakis and Mayer 1996).....	26
Table 5: The properties of the Herbsstrasse.....	31
Table 6: Timetable of simulation	36
Table 7: Average difference PET and air temperature on three receptors on 19.08.2012	53
Table 8: Average difference PET and air temperature on three receptors on 20.08.2012	55
Table 9: Average difference PET and air temperature on three receptors on 21.08.2012	75

7.3 List of Equations

UHI Intensity (1)	6
Energy balance for human body (2).....	28

8 LITERATURE

8.1 Reference

Akbari, H. and Rose, L.S., 1999. Characterizing the Fabric of the Urban Environment: A Case Study of Sacramento, California. Berkeley, CA, Lawrence Berkeley National Laboratory: 48.

Akbari, H., Menon, S. and Rosenfeld, R., 2008. Global cooling: increasing world-wide urban albedos to offset CO₂. 4 September.

Akbari, H., 2005. Energy Saving Potentials and Air Quality Benefits of Urban Heat Island Mitigation: Heat Island Group Lawrence Berkeley National Laboratory (510) 486-4287.

American Meteorology Society 2012.

<http://glossary.ametsoc.org/w/index.php?title=Special%3ASearch&search=Urban+heat+island&fulltext=Search> . Accessed 5.25.2015.

Arnfield, A.J., 2003. Review two decades of urban climate research: a review of turbulence, exchange of energy and water, and the urban heat island. International of climatology 23, pp.1-26. DOI: 10.1002/joc.859.

Asaeda, T. Ca, V.T. and Wake, A. 1996. Heat storage of pavement and its effect on the lower atmosphere. Atmospheric environment 30(3), pp. 413-427.

ASHRAE 2001: Chapter 8-Comfort. In Handbook of Fundamentals. American Society For heating Refrigerating and Air Conditioning, Atlanta: 8.1-8.29.

ASHRAE 2005. Chapter 16- Airflow around buildings. Atlanta, GA: ASHRAE

Bass, B. , Kravenhoff, S , Martilli, A. and Stull, R., 2002. Mitigating the Urban Heat Island with Green Roof Infrastructure. Toronto, North American Urban Heat Island Summit, Toronto Atmospheric Fund.

Baely, W.G. (Ed), 1997. The surface Climate of Canada .Canada.

BerkeleyLab. <http://newscenter.lbl.gov/2012/09/13/parking-lot-science/> Accessed 14.07.2015.

Berkeley Lab. <https://heatisland.lbl.gov/> . Accessed 12.07.2014.

Bruse, M. 1999. ENVI-MET Model Architecture. Accessed 15, 2014, from <http://www.envi-met.com/>

- Chen, L. and Ng, E. 2011. Outdoor thermal comfort and outdoor activities: A review of research in the past decade. Elsevier Journal 19 September, pp. 118-125. DOI:10.1016.
- Encyclopædia Britannica Online, s. v. planetary boundary layer (PBL), accessed Mai 20, 2015, <http://www.britannica.com/EBchecked/topic/1364303/planetary-boundary-layer-PBL>.
- EPA, 2008. Reducing Urban Heat Islands: Compendium of Strategies Urban Heat Island Basics. October 2008.
- Erell, E., Pearlmutter, D. and Williamson, T., 2011. Urban Microclimate- Designing the space Between the building 1st ed. London, Washington, DC: Earthscan.
- Fanger, P.O., 1970. Thermal comfort in Buildings with Low. Energy Cooling. Danish Technical Press. Copenhagen, Submitted by Technical University of Denmark, 1.17 May 2009.
- Fietsberaad crow 2011.
<http://www.fietsberaad.nl/?section=Voorbeeldenbank&lang=en&ontwerpvoorbeeldPage=Voorrangskruispunten&mode=detail&repository=Left-turn+provision+for+cyclists>. Accessed 6.10.2015
- Furth, 2012.
http://wiki.coe.neu.edu/groups/nl2011transpo/wiki/794d3/14_Red_Asphalt_Pavement.html. Accessed 22.09.2014.
- Garden Punk, 2012. <http://gardenpunk.wordpress.com/2012/06/04/how.plants.drink/> . Accessed 22.09.2014.
- Gartland, L., 2008. Heat Island: understanding and mitigation heat in urban areas. London sterling VA: 2008.
- Gartland, L., 2001. Cool Roof Energy Savings Evaluation for City of Tucson Thomas .Price Service Center Administration Building One. Tucson, AZ, City of Tucson.
- Givoni B., 1976. Man, Climate and Architecture. Van Nostrand Reinhold. New York.
- Green Business watch, <http://greenbusinesswatch.org/blog/green-roof-images>. Accessed 6.10.2015.
- Googlemap, 2014.
<https://www.google.at/maps/place/Herbststra%C3%9Fe,+1160+Wien/@48.2060242,16.3315011,197m/data=!3m1!1e3!4m2!3m1!1s0x476d07fcc92c5bf:0x4af632730606ba93>. Accessed 15.04.2014.

- Hakim, A. A., Petrovitch, H., Burchfiel, C. M., Ross, G. W., Rodriguez, B. L. and White, L. R., 1998. Effects of walking on mortality among nonsmoking retired men. *New England Journal of Medicine*, 338, pp. 94–99.
- Hass-Klau, C., 1993. Impact of pedestrianisation and traffic calming on retailing: A review of the evidence from Germany. *Transport Policy*, 1(1), pp.21–31.
- Haus und Wohnen, http://www.haus-und-wohnen.ch/de/garten_pools/garten_trends/planung_gestaltung/entries/110819_boden-waende-mauern-wege.php . Accessed 6.10.2015.
- Heat Island Group, Lawrence Berkeley National Laboratory: <https://heatisland.lbl.gov/>. Last accessed 10.07.2015.
- Honjo, T., 2009. Thermal comfort in outdoor Environment: Global Environmental Research. Japan, 23 March, 2009, pp.43-47.
- Höppe, P., 1993. Heat balance modelling. *Experientia* 49, pp. 741–746.
- Höppe, P., 1999. The physiological equivalent temperature – a universal index for the biometeorological assessment of the thermal environment. *Int J Biometeorol* 43, pp. 71–75.
- Huang, J. and Akbari, H., 1990. The wind-shielding and shading Effects of Trees on Residential Heating and Cooling Requirements. ASHRAE Winter Meeting, Atlanta, Georgia, American Society of Heating, Refrigerating and Air-Conditioning Engineers.
- Kiesel, K., Vuckovic, M., Orehounig, K. and Mahdavi, A. 2012. Analysis of micro climatic variations and the urban heat island phenomenon in the city of Vienna. *EURA, Urban Europe – Challenges to Meet the Urban Future*, Vienna, Austria, and September 20-22.
- Jacobs, J., 1972. *The death and life of great American cities*. Harmondsworth: Penguin.
- Lebens, M., 2012. Porous Asphalt Pavement Performance in Cold Region: Office of Materials and Road Research Minnesota Department of Transportation. April 2012.
- Lindberg, F. 2007. Modelling the urban climate using a local governmental geo-database. Meteorological application. Volume 14, 2007, pp. 263-273. DOI: 10.1002/met.299.
- Magli, S., Lodi, C., Lomboroso, L. Muscio, A. and Teggi, S. 2014. Analysis of the urban heat island effects on building energy Consumption. *Int J Energy Environ Eng*, 2015, pp. 91–99. DOI: 10.1007/s40095-014-0154-9.

- Mahdavi, A., Kiesel, K. and Vuckovic, M. 2014. Empirical and computational assessment of the urban heat island phenomenon and related mitigation measures. NSB 2014, 10th Nordic Symposium on Building Physics, Lund, Sweden, June 15-19.
- Matzarakis, A. and Amelung, B., 2008. Physiological Equivalent Temperature as Indicator for Impacts of Climate Change on Thermal Comfort of Humans. *Seasonal Forecasts, Climatic Change and Human Health: Health and Climate Volume 30*, pp. 161-.172.
- Matzarakis, A. and Mayer, H., 1996. Another kind of environmental stress: Thermal stress. WHO collaborating center for Air Quality Management and Air pollution Control. *NEWSLETTERS 18*, 7–10.
- Matzarakis, A. and Mayer H., 1999. Application of universal thermal index: physiological equivalent temperature. *Biometeorology Journal*. pp. 76-84.
- McPherson, E.G. and Simpson, J. R., 1999. Reducing Air Pollution through Urban Forestry. 48th Annual Meeting of the California Forest Pest Council, Sacramento,CA, 18–19 November.
- Medgar, L. Marceau and Martha, G., 2007. Solar Reflectance of Concretes for LEED Sustainable Sites Credit: Heat Island Effect. Portland Cement Association 2007.
- Meier, A., 1990. Measured Cooling Saving from vegetative Efficiency in Building, Pacific Grove,CA, American Council for an Energy Efficient Economy.
- Met office, 2011. National Meteorological Library and Archive. Fact sheet 14 - Microclimates version 01.
- Mills G., 1999. Urban climatology and urban design. ICB-ICUC; Sydney, Australia. PP. 541-544.
- Mirzaei, P. and Haghighat, F., 2010. Approaches to study urban Heat Island-Abilities and limitation. *ELSEVIER Journal of the Building and Environmental 45*, pp. 2192-2201.DOI:10.1016/J.buildenv.2010.04.001.
- Moll, G. and Berish, C., 1996. Atlanta's changing environment. *American Forests Spring*: 26–29.
- Morris, C. J.G. and Simmonds, I. 2000. Associations between varying magnitudes of the urban heat island and the synoptic climatology in Melbourne, Australia'. *International Journal of Climatology 20*, pp. 1931–1954.
- Munn, T. (Ed.), 2001. *Encyclopedia of Global Environmental Change*, 5 Volume Set, Encyclopedia of Global Environmental Change.

NUKE, CZ.2001. [HTTP://WWW.ABOUT.GARDEN.COM/EI/EN/00474.01.EUROPEAN.LARCH/](http://www.about.garden.com/ei/en/00474.01.european.larch/). Accessed 29.09.2014.

OBI, <http://www.obi.de/de/rat-und-tat/wissenswertes/rasengittersteine/index.html>. Accessed 6.10.2015.

Official Website of the Unified Government of Wyandotte Country and Kansans City,2011. http://www.wycokck.org/InternetDept.aspx?id=23020&menu_id=1444&banner=15284. Accessed 01.08.2014.

Oke, T. R., 1969. Towards a more rational understanding of the urban heat island. McGill University Climatological Bulletin. Volume 5, pp. 1-20.

Oke, T.R., 1982. The energetic basis of the urban heat island. Quarterly journal of the Meteorological Society 108 (455), pp. 1-24. DOI:10.1002/qj.49710845502.

Oke , T.R., 1987. Boundary layer climates.2nd ed.England

Oke, T.R., 1988. Street design and urban canopy layer climate," Energy and Buildings, (11), pp.103–113.DOI: 10.1016/0378-7788(88)90026-6

Oke, T.R., 1997. Urban environments. In: The Surface Climates of Canada (W.G. Bailey, T.R. Oke and W.R. Rouse, eds). McGill-Queen's University Press, Montreal, pp. 303–327

Oke, T.R., 2005. Towards better scientific communication in urban climate. Department of geography, University of British Columbia, Vancouver, B.C.Canada, pp. 179-190. DOI:10.1007/s00704.005.0153.0

Oke, T.R., 2008. The energetic basis of the urban heat island. Quarterly Journal of the Royal Meteorological Society, Volume (108), January 1982, pp. 1–24. DOI: 10.1002/qj.49710845502 .

Pomerantz , M. Pon, B. Akbari, H. and S.C. Chang., 2000. The effect of pavement Temperatures on air temperatures in large cities. Berkeley, CA, Lawrence Berkeley National Laboratory: 20

Population Reference Bureau., 2005. World population Data Sheet. Population Reference Bureau; 2005.

SAFE GURD, 2012. http://www.safeguardeurope.com/applications/green_roofs_flat.php. Accessed 18.08.2014.

Taha, H., 1997. Urban climates and heat islands: albedo, evapotranspiration, and anthropogenic heat. Energy and Buildings, Volume 25, pp. 99-103.

Toudert, A., 2005. *Dependence of Outdoor Thermal Comfort on Street Design in Hot and Dry Climate*. Case Study: Germany. PhD dissertation: University of Freiburg.

UHI, 2014. <http://eu.uhi.eu/>. Accessed 25.07.2014.

Urban, B. and Roth, K., 2010. Guidelines for Selecting Cool Roofs: Building Technology Program. Department of Energy Building Technologies Program and Oak Ridge National Laboratory, July 2010, U.S., pp. 1-23.

Variety of Life, 2014. http://taxondiversity.fieldofscience.com/2014_08_01_archive.html . Accessed 18.08.2014.

Verein Deutscher Ingenieure. 1998. VDI 3787, Part I: environmental meteorology, methods for the human-biometeorological evaluation of climate and air quality for the urban and regional planning at regional level. Part I: climate. VDI/DIN-Handbuch Reinhaltung der Luft, Band 1b, Düsseldorf, pp. 29.

Voogt, J. A. 2002. Urban Heat Island. Encyclopedia of Global Environmental Change. Volume 3, pp. 660-666.

Vuckovic, M., Kiesel, K. and Mahdavi, A. 2014. The sources and implications of urban climate variance in Vienna. 3rd International Conference on Countermeasures to Urban Heat Island, Venice, Italy, October 13-15.

Whyte, W. H., 1988. *City: Rediscovering the center*. New York: Doubleday.

Wilby, R. L., Jones, P. D., Lister, D. H., 2011. Decadal variations in the nocturnal heat island of London. *Weather*, Volume 66, Issue 3, pp. 59-64.

APPENDIX

8.2 Abbreviation

ACC	Asphalt Cement Concrete
AKH	Allgemeines Krankenhaus
ASHREA	American Society of Heating, Refrigerating and Air conditioning Engineers
C	Convective Heat Flow
CFD	Computational Fluid Dynamic
ED	Latent Heat flow to evaporate water diffusing through the skin
ET	Effective Temperature
ER _e	sum of heat flows for heating and humidifying the inspired air
ES _w	Heat Flow due to evaporation of sweat
FA	Free Atmosphere
HOP	Humid Operative Temperature
HSI	Heat Streets Index
ITS	Index of Thermal Stress
M	Metabolic Rate
MEMI	Munich Energy Balance Model for Individual
ML	Mixing Layer
OP	Operative Temperature
OUT_SET	Out Standard Effective Temperature
PBL	Planetary Boundary layer
PET	Physiological Equivalent Temperature
PMV	Predict Mean Vote
PCC	Portland cement concrete
PT	perceived Temperature
R	Net Radiation
S	Storage Heat Flow for Heating or Cooling the Body Mass

SL	Surface Layer
UBL	Urban Boundary Layer
UCL	Urban Canopy Layer
UHI	Urban Heat Island
UML	Urban Mixing Layer
URS	Urban Roughness Sub layer
UV	Ultraviolet
W	Physical Work Put

8.3 Day 3

8.3.1 Basic Model (without mitigation)

This scenario consisted of buildings with plastered walls, tiled roofs and asphalt for pedestrian and street area. The purpose of this model was to assess the most appropriate base model to run the envisioned mitigation scenarios. Once the simulation data was compared to the measured one (Figure 56), a significant difference was not apparent. Therefore, the model was deemed acceptable for the ongoing study.

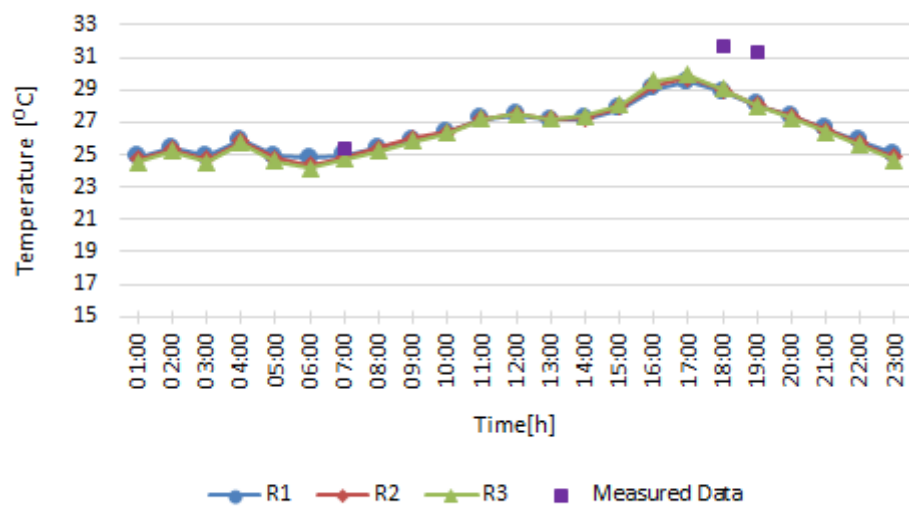


Figure 56: Simulated air temperature of BC Model on 21.08.2012

Figure 57 shows the average air temperature sampled from the three receptors, for all four models. The results show that the effects of combined mitigation strategies result in slight air temperature reduction when compared to the basic model. This is further seen in all scenarios. However, the highest offset is observed during the morning and late afternoon hours. This reduction can be as high as 0.5 K.

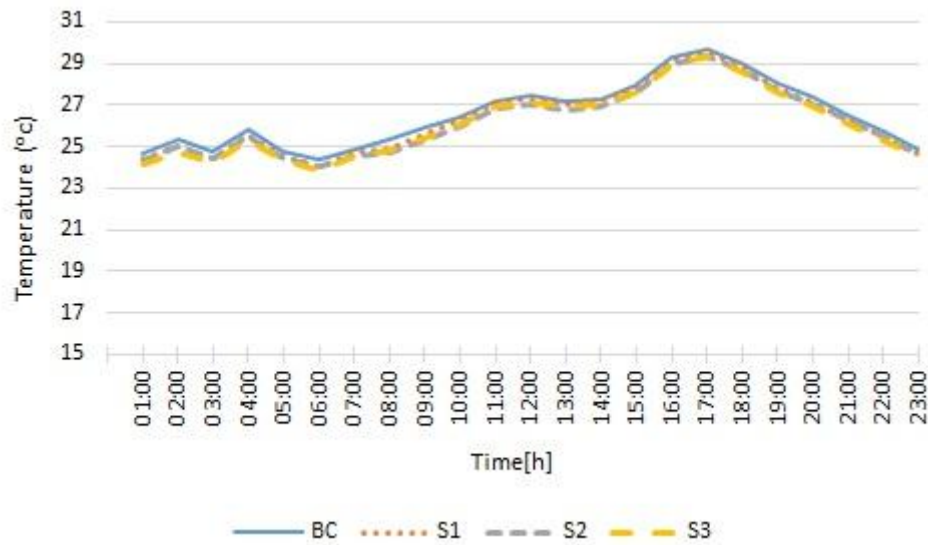


Figure 57: Simulated average air temperature on 21.08.2012

8.3.2 Physiological Equivalent Temperature on the Third Day

Figure 58 shows the distribution of PET for each receptor of the basic model. It can be clearly seen that the difference of PET for the receptors 2 and 3 are larger than the receptor 1.

As noted in the previous day, during early morning hours considerable higher PET was measured for all three receptors, which again may be attributed to the specific geometry and higher exposure to the incoming solar radiation (as seen from T_{mrt} values in Figure 59).

However, these differences are smaller when the mitigation scenarios S1, S2 and S3 are applied (as seen in Figures 60 to 62). Furthermore, the effects on the outdoor thermal comfort are found to be higher.

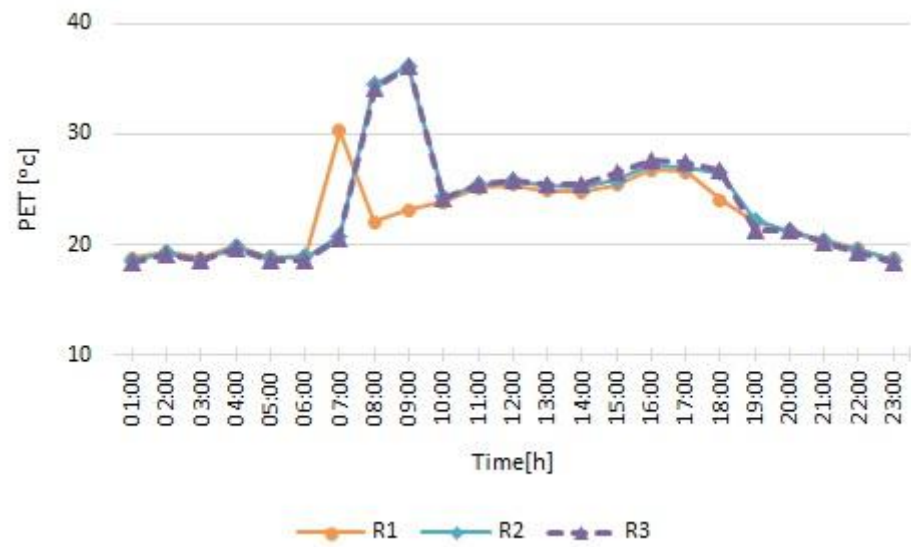


Figure 58: Physiological equivalent temperature of the BC on 21.08.2012

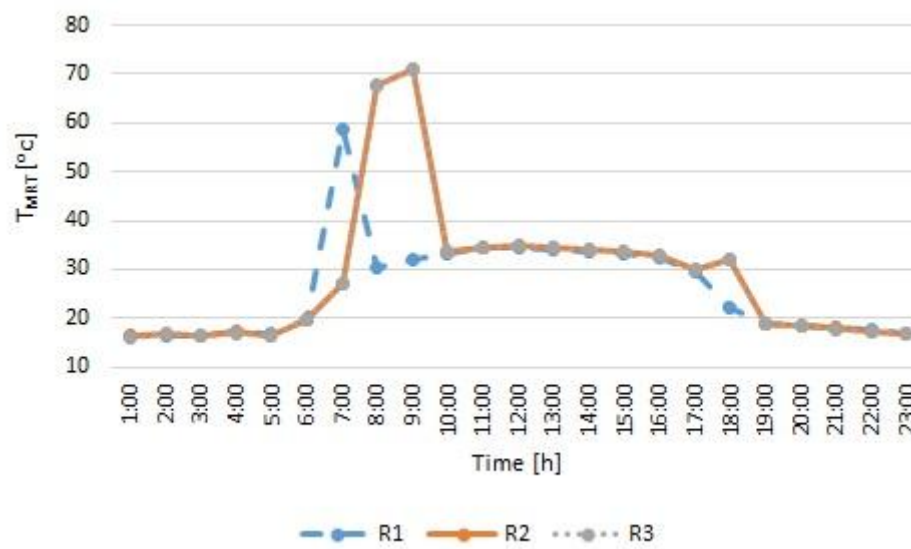


Figure 59: Mean Radiant Temperature of the BC on 21.08.2012

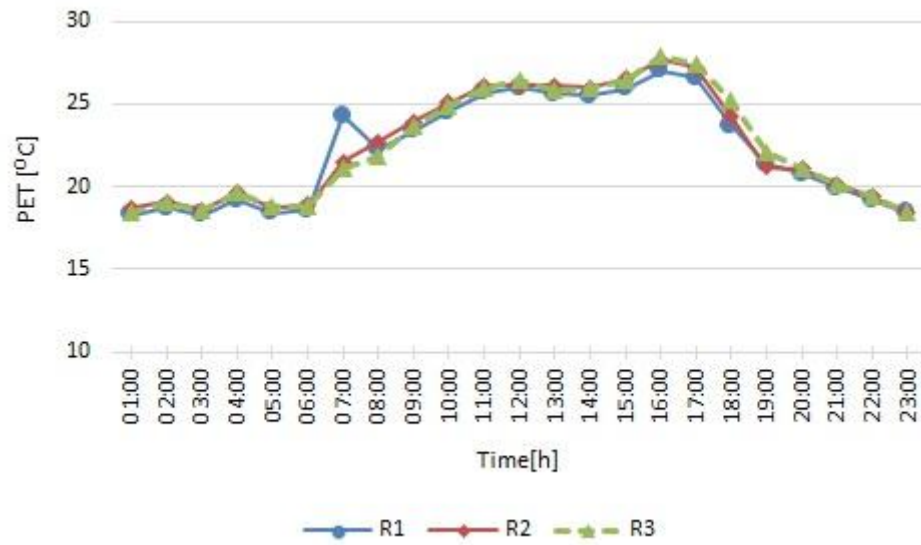


Figure 60: Physiological equivalent temperature of the S1 on 21.08.2012

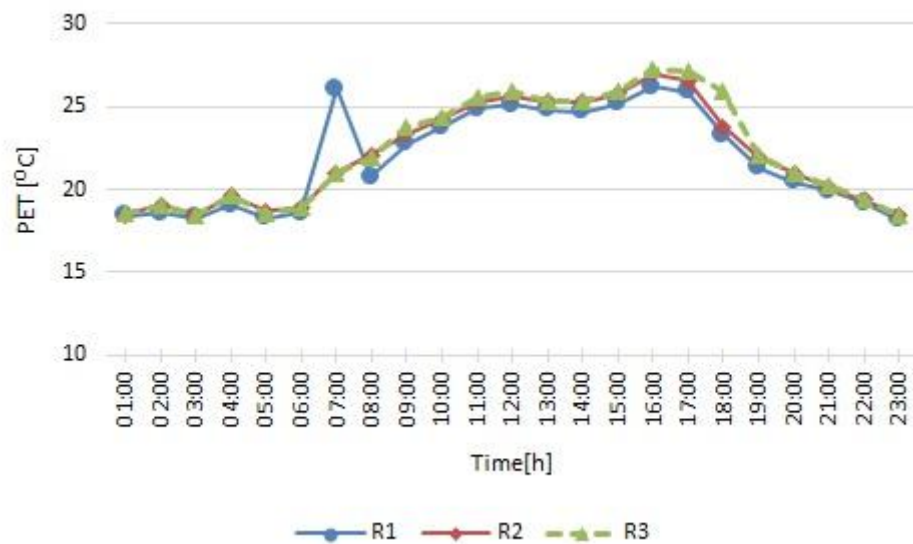


Figure 61: Physiological equivalent temperature of the S2 on 21.08.2012

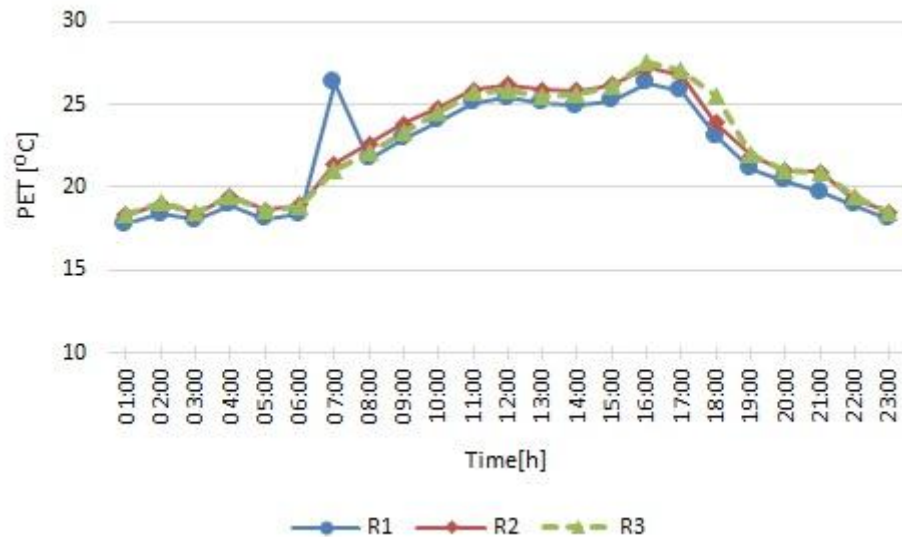


Figure 62: Physiological equivalent temperature of the S3 on 21.08.2012

8.3.3 Average Difference air temperature between BC and S1-S2-S3

The figure 63 shows the difference in air temperature between BC and three scenarios (S1, S2, and S3) on 21.08.2012. It can be observed that Scenarios 2 and 3 resulted in approximately equal reduction of air temperature, however, displayed in different time. The cooling effect of Scenarios 2 was more pronounced during the daytime, while the Scenarios 3 was proven more effective during the nighttime. Scenario 2 shows the greatest daytime reduction of air temperature, in range of 0.3K to 0.6K. The peak reduction was noted during the early morning hours, but lasting only for 3 hours. Scenario 3 shows that the air temperature reduction achieved was about 0.6 K. However, even if the peak reduction was smaller than that noted in Scenario 2, the time frame was longer. In general, Scenario 1 was proven to be the least effective of all interventions analyzed, and especially during the daytime. During the nighttime, the mitigation effect was noticeably improved. It can be further concluded that the Scenario 3 proved to be the most beneficial.

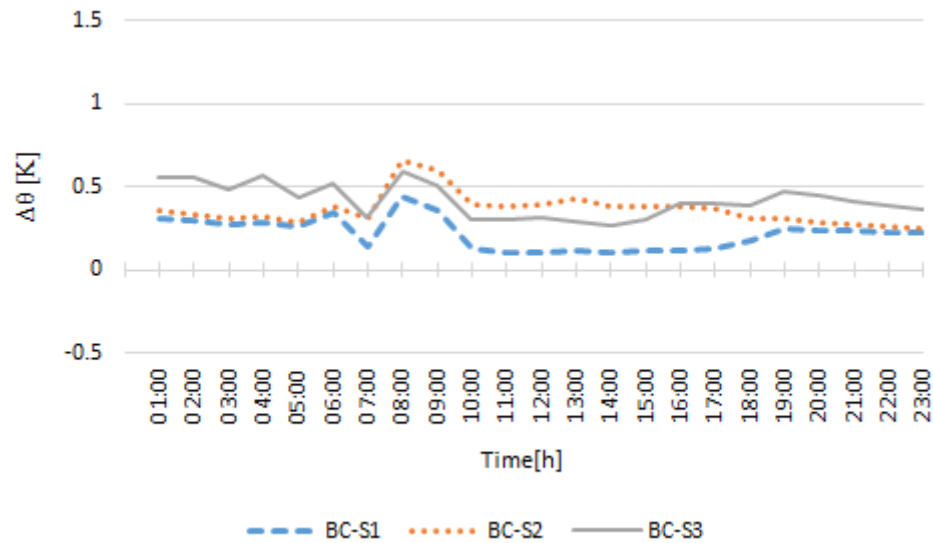


Figure 63: Average differenced air temperature between BC and S1-S2-S3 on 21.08.2012

8.3.4 Compared PET between BC and S1-S2-S3

Figure 64 shows the output PET values collected at one receptor (R3) for all four models (BC, S1, S2, and S3). In general, it can be observed that the most pronounced PET reduction was during the early morning (from 06:00 until 10:00) and late afternoon hours (from 17:00 until 19:00). This circumstance might be due to the overall higher solar gain noted in this particular time, resulting in increased mean radiant temperature of the Base Case. However, during the daytime, the PET of Base Case decreased dramatically, which might be due to the sudden cloud cover forming over the area. During the remaining hours, the PET curve resulting from envisioned scenarios followed the one from the Base Case. However, it can be said that Scenarios 2 and 3 performed better than Scenario 1, resulting in an offset of around 1K between the respective lines. Additionally, this circumstance was more pronounced during the daytime, when the average reduction was found to be the greatest.

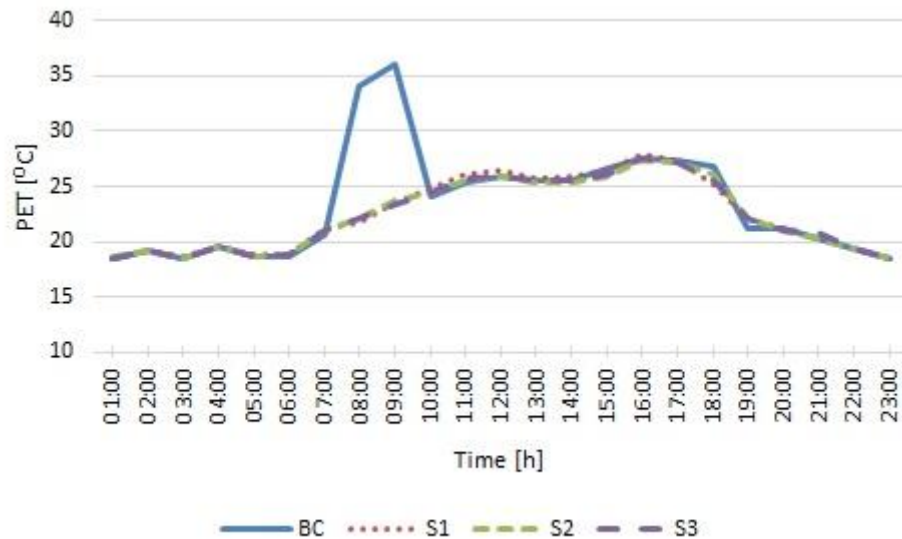


Figure 64: Compared the average PET between four Models on 21.08.2012 at R3

Table 9 shows the average difference of PET values collected from three receptors of basic models and three scenarios, respectively. As it can be seen from the table, the average PET between BC-S1 is 0.75 K and between BC-S2 and BC-S3 is 1.01 K and 0.93 K. Therefore, Scenario 2 was proven to be the most effective in terms of the improved outdoor thermal comfort, whereas Scenario 3 displayed the highest reduction of air temperature.

Table 9: Average difference PET and air temperature on three receptors on 21.08.2012

Date	Scenarios	ΔPET [K]			ΔT [K]		
		R1	R2	R3	R1	R2	R3
21.08.2012	BC-S1	0.32	0.99	0.95	0.41	0.19	0.06
	BC-S2	0.65	1.31	1.07	0.56	0.33	0.2
	BC-S3	0.67	1.09	1.05	0.74	0.37	0.15